J. Fluid Mech. (1987), *vol.* 176, *pp.* 1–31
Printed in Great Britain

Rivulet instabilities

By GERALD W. YOUNG† AND STEPHEN H. DAVIS

Department of Engineering Sciences and Applied Mathematics, Northwestern University, Evanston, IL 60201, USA

(Received 17 April 1985 and in revised form 16 June 1986)

We examine a three-dimensional rivulet flowing down a vertical plane. There exists a basic state with fully developed, unidirectional flow and straight contact lines. In the absence of contact-angle hysteresis the slope of the contact angle versus contact-line speed relationship measures the mobility of these contact lines. The stability characteristics of flat rivulets subject to long wave disturbances are examined using lubrication theory. We find that kinematic-wave instabilities are predicted for wide rivulets or rivulets with rather immobile contact lines, while capillary break-up is predicted for narrower rivulets with mobile contact lines. We find for all cases that the expression for the growth rate depends weakly on slip between the liquid and solid near the contact line, but strongly on the shape of the rivulet and the mobility of the contact lines. We discuss in detail the mechanisms by which the contact lines affect the instabilities.

1. Introduction

A rivulet is a stream of liquid flowing down a solid surface and sharing an interface with a surrounding gas. A simple example of a rivulet is a stream of water seen on the windshield of a car after a rainfall.

Rivulets occur in a wide variety of engineering applications. Drops rolling off a surface used for condensation may coalesce, forming a rivulet. Rivulets arise in the melting and casting of metals. In processes of heat exchange and gas absorption, rivulets play a major role since they have a large surface area to cross-sectional area ratio. This allows for enhanced heat transfer. In industrial coating processes using liquid layers, the film may become unstable, breaking up into rivulets. In all of the above areas, a knowledge of the fluid motion and stability characteristics of rivulet flow is required to assess the efficiency of the process.

As shown in figure 1, a rivulet has two contact lines. The motions of these contact lines can give rise to rivulets with many different geometrical configurations. The simplest of these is the straight rivulet considered by Towell & Rothfeld (1966). This is a rivulet with straight, parallel contact lines whose flow is steady, fully developed and unidirectional. The interface forms a cylindrical meniscus. Such rivulets exhibit a wide variety of instabilities. Kern (1969, 1971, 1975 unpublished) and Culkin (1981) see the break-up of straight rivulets into drops, rivulet meandering, formation of large amplitude surface waves, and the transition of rivulet flow from laminar to turbulent regimes. Our work will concentrate on the break-up and surface-wave instabilities. These two features of rivulet flow tempt one to classify rivulets somewhere in between capillary jets and film flows. It is not surprising that rivulets are susceptible to a dropwise break-up since they possess a curved meniscus as discussed by Davis

† Present address: Department of Mathematics, University of Akron, Akron, OH 44325, USA.

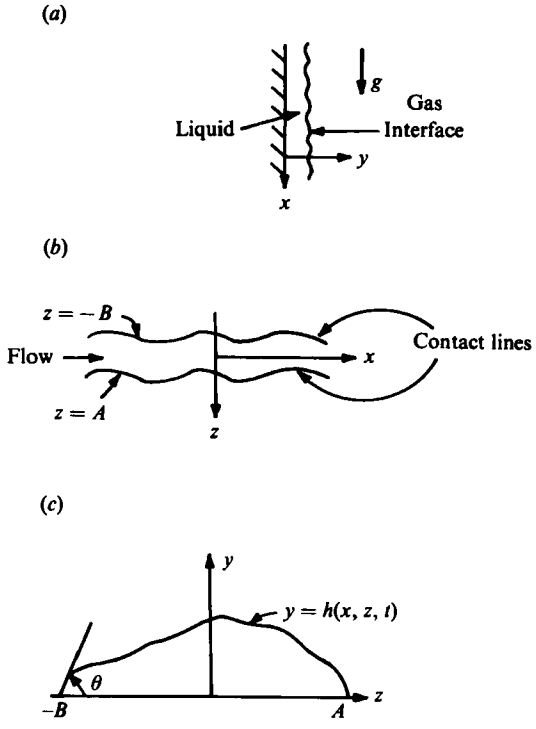

FIGURE 1. Sketch of a rivulet flowing down a vertical wall: (*a*) side view; (*b*) top view; (*c*) front view.

(1980). This curvature allows for a capillary instability (Rayleigh 1879) where surface tension causes capillary pressure gradients which force fluid from thinner to thicker regions. On the other hand, wide rivulets with flat interfaces clearly resemble films. It is well known (Benjamin 1957; Yih 1963) that films are susceptible to kinematic-wave instabilities. Thus, one also expects surface waves to develop on rivulets.

The goal of the present work is to investigate the break-up and kinematic-wave instabilities for the purpose of further determining the effects of the presence of contact lines and boundary conditions posed there. As previous studies of flows with moving contact lines have shown [see Dussan V. & Davis 1974; Dussan V. 1976; Greenspan 1978, for example], it is convenient to allow the fluid to slip along the solid surface in the vicinity of the contact line; this suppresses the non-integrable stress singularity that would otherwise appear. In addition one must pose boundary conditions at the contact line in order that there be a mathematically well-posed problem which leads to physically realistic results. The following three types are most often posed:

(i) condition of contact,

(ii) condition of contact angle changing with contact-line speed, and,

(iii) condition of bounded velocity at the contact line.

The first of these defines where the interface contacts the solid surface. As discussed by Young (1985), the last states that the contact line is a fluid boundary. The second is usually posed as the form $\theta = G(U_{\mathrm{CL}})$ where θ is the angle measured from the solid surface to the interface at the contact line, and U_{CL} is the speed of the contact line measured relative to the speed of the surface. The function G is usually chosen to

describe experimental observation. The most common forms of G (Davis 1980) represent contact-angle hysteresis, fixed contact lines, fixed contact angle, and smooth contact angle variation. The slope $G'(0)$, when it exists, measures the mobility of the contact line whereas the static contact angles measure the wetting characteristics of the solid.

There has been one previous theoretical analysis (Weiland & Davis 1981) of dynamic rivulet instabilities. However, their formulation appears to be incomplete in that they do not pose the boundedness condition. Thus they need to introduce ad hoc procedures to determine unknown constants of integration.

We begin by formulating the problem for flow of a rivulet down a vertical plate. We allow slip between the liquid and the solid at the contact line by posing a slip condition similar to that of Greenspan (1978). We assume a linear relationship *without hysteresis* between the speed of the contact line and the contact angle. The slope $G'(0)$ of the advancing and receding portions of this relationship may take on values from zero to infinity so that the contact-line motion can vary from fixed-contact-angle to fixed-contact-line regimes. Thus we can determine the effects of the mobility of the contact lines.

The system governing the above is then non-dimensionalized. The streamwise and normal coordinates are scaled on the rivulet height while the cross-stream coordinate is scaled on half the rivulet width. It is assumed that long-wave disturbances are present so that a non-dimensional wavenumber k, and aspect ratio δ result.

We discuss a linearized instability of the straight rivulet for k and δ small. In order to do asymptotics in two small parameters, we assume that k and δ are related through an expression of the form

$$\delta^2 = O(k^s). \tag{1.1}$$

By varying s from 0 to ∞ we can allow the rivulet to widen to the extreme case of film flow. We perform the analysis for various values of s in relation (1.1) to determine the effects of the width of the rivulet on the stability characteristics. We compare our results with the experimental observations of Kern (1969, 1971, 1975 unpublished) and Culkin (1981). Finally, we discuss the mechanisms by which the contact lines affect the stability characteristics of rivulets. The importance of these mechanisms is measured by a parameter G_1, proportional to

$$\frac{G'(0)}{\delta^2}, \tag{1.2}$$

which is a ratio of the mobility of the contact lines to the square of the width of the rivulet.

2. Formulation

Consider a rivulet flowing down a long, smooth, vertical plate as shown in figure 1. The rivulet consists of a Newtonian fluid which has a constant density ρ and a constant viscosity μ. The surrounding fluid is a passive gas with a constant pressure, which we take equal to zero. The entire system is isothermal.

The governing equations for the system are the Navier–Stokes equations and the continuity equation:

$$\rho(u_{i_t} + u_j u_{i,j}) = \sigma_{ij,j} + \rho F_i \tag{2.1}$$

and

$$u_{i,i} = 0, \tag{2.2}$$

where u_i is the velocity vector $(u_i) = (u, v, w)$, σ_{ij} is the stress tensor,

$$\sigma_{ij} = -p\delta_{ij} + \mu(u_{i,j} + u_{j,i}), \tag{2.3}$$

and F_i is the gravity force per unit mass,

$$(F_i) = (g, 0, 0). \tag{2.4}$$

The above equations refer to a right-handed Cartesian coordinate system whose origin is on the plate, whose x-axis points down the plate and whose y-axis points normal to the plate into the liquid, as shown in figure 1.

There are boundary conditions appropriate to the liquid–gas interface at $y = h(x, z, t)$. These are the kinematic condition

$$v = h_t + uh_x + wh_z, \tag{2.5}$$

and the stress balances

$$\sigma_{ij} n_j n_i = 2HT, \tag{2.6}$$

$$\sigma_{ij} n_j t_{1i} = 0, \tag{2.7}$$

$$\sigma_{ij} n_j t_{2i} = 0. \tag{2.8}$$

The first of these states that the interface is a bounding surface between the fluid and the gas, while the stress balances give the normal-stress jump across an interface with constant surface tension T, and zero tangential shear stress, respectively. Here $\boldsymbol{n}$ is the unit outward normal vector to the interface,

$$\boldsymbol{n} = (-h_x, 1, -h_z)(1 + h_x^2 + h_z^2)^{-\frac{1}{2}}, \tag{2.9}$$

$\boldsymbol{t}_1$ and $\boldsymbol{t}_2$ are orthogonal unit tangent vectors

$$\boldsymbol{t}_1 = (0, h_z, 1)(1 + h_z^2)^{-\frac{1}{2}}, \tag{2.10}$$

$$\boldsymbol{t}_2 = \boldsymbol{n} \times \boldsymbol{t}_1, \tag{2.11}$$

and H is the mean curvature of the interface,

$$2H = [h_{xx}(1 + h_z^2) - 2h_x h_z h_{xz} + h_{zz}(1 + h_x^2)](1 + h_x^2 + h_z^2)^{-\frac{3}{2}}. \tag{2.12}$$

There are boundary conditions appropriate to the solid–liquid interface. Dussan V. & Davis (1974) have shown that the no slip condition $u_i = 0$ on $y = 0$, together with the movement of the contact line result in a multi-valued velocity field at the contact line. This corresponds to a non-integrable stress singularity giving an unbounded force at the contact line. This theoretically unreasonable result can be relieved by allowing perfect slip on the fluid–solid interface near the contact line. We follow Greenspan (1978) and pose a slip model:†

$$u = \frac{\alpha}{h} u_y, \quad v = 0, \quad w = \frac{\alpha}{h} w_y \quad \text{on } y = 0. \tag{2.13a, b, c}$$

The liquid is allowed to slip over the solid plate at a speed directly proportional to the shear. We choose α to be a numerically small constant so that the magnitude α/h of the slip, is significant only near the contact line where $h = 0$.

There are boundary conditions at the contact lines. Since the contact-line positions, given by $z = A(x, t)$ and $z = -B(x, t)$ are themselves unknown, we must pose conditions on the motion of these lines.

First, there are the conditions of contact,

$$h = 0 \quad \text{at } z = A, \tag{2.14a}$$

$$h = 0 \quad \text{at } z = -B. \tag{2.14b}$$

† One should really allow slip only normal to the contact line. The model (2.13) results in an $O(\alpha)$ slip along the rivulet axis, which, though non-zero, is small. We choose form (2.13) for convenience.

Second the velocity field at the contact lines is assumed to be bounded. This condition is *implicit* in the models of moving contact lines considered to date (e.g. Greenspan 1978; Hocking 1983; Dussan V. & Chow 1983).

Third, the contact angle† depends on the contact-line speed. We define the contact angle θ such that its tangent is the slope of the interface at the contact line in the direction $\boldsymbol{\nu}$ normal to the contact line. Thus,

$$\tan\theta_A = -\nabla h\cdot\boldsymbol{\nu}_A = -h_z(A_x^2+1)^{\frac{1}{2}} \quad \text{at } z=A, \tag{2.15a}$$

$$\tan\theta_B = -\nabla h\cdot\boldsymbol{\nu}_B = h_z(B_x^2+1)^{\frac{1}{2}} \quad \text{at } z=-B. \tag{2.15b}$$

We consider contact lines that exhibit no contact-angle hysteresis. For simplicity only we consider a piecewise linear model, namely

$$\theta = G(U_{\mathrm{CL}}) = \phi + G'(0)\,U_{\mathrm{CL}}. \tag{2.16}$$

Equation (2.16) possesses two special cases. (i) If $G'(0)\to\infty$, then $U_{\mathrm{CL}}\to 0$ and the contact line is stationary. Thus, for *fixed contact lines*, A and B are time-independent. (ii) If $G'(0)\to 0$, then $\theta\to\phi$ for all time and the dynamic angle equals the static angle always. This is the *fixed-contact-angle* case. Generally, $0 < G'(0) < \infty$ and we have *smooth contact-angle variation*. We also note here an equivalent form for the kinematic boundary condition (2.5) which follows from integrating the continuity equation across the thickness of the rivulet

$$h_t + \frac{\partial}{\partial x}\int_0^h u\,\mathrm{d}y + \frac{\partial}{\partial z}\int_0^h w\,\mathrm{d}y = 0. \tag{2.17}$$

This form will be convenient for the linear stability analysis to follow.

3. Scaling

We follow Weiland & Davis (1981) and scale all variables for the analysis of long waves with wavelength λ on shallow rivulets of width $2L$. This analysis will then apply to rivulets with small contact angles. If d is the maximum height of the rivulet, then we have two small parameters, the wavenumber k,

$$k = \frac{2\pi d}{\lambda}, \tag{3.1}$$

and the aspect ratio δ,

$$\delta = \frac{d}{L}. \tag{3.2}$$

We define the velocity scale U_{s}

$$U_{\mathrm{s}} = \frac{\rho g d^2}{\mu}, \tag{3.3a}$$

the pressure scales p_{s},

$$p_{\mathrm{s}} = \frac{\mu U_{\mathrm{s}}}{d}, \tag{3.3b}$$

and the timescale t_{s},

$$t_{\mathrm{s}} = \frac{d}{U_{\mathrm{s}}}. \tag{3.3c}$$

† The angle θ would depend on speed if attachment or detachment kinetics of the liquid from the solid has timescales comparable to those of the flow. Ngan & Dussan V. (1982) observe θ_{APP}, which coincides with θ for small speeds, that show variations with speed. Hocking (1983) conjectures that (in the absence of kinetic effects) θ would be constant.

The scaled quantities, denoted by upper-case letters, are as follows:

$$\left.\begin{aligned} X &= \frac{2\pi x}{\lambda}, \quad Y = \frac{y}{d}, \quad Z = \frac{z}{L}, \quad T = \frac{2\pi U_s}{\lambda} t, \\ U &= \frac{u}{U_s}, \quad V = \frac{v}{kU_s}, \quad W = \frac{\lambda w}{2\pi L U_s}, \quad P = \frac{kp}{p_s}, \\ h' &= \frac{h}{d}, \quad A' = \frac{A}{L}, \quad B' = \frac{B}{L}. \end{aligned}\right\} \tag{3.4}$$

The scaling gives rise to the following non-dimensional groups:

$$\left.\begin{aligned} R &= \frac{\rho^2 g d^3}{\mu^2} \\ B_d &= \frac{\rho g d^2}{T} \\ \kappa &= \alpha/d^2 \end{aligned}\right\} \tag{3.5}$$

where R is the Reynolds number, κ is the slip coefficient and B_d is a Bond number based on the height of the rivulet. In addition it is convenient to introduce the Bond number B_L based on the width of the rivulet

$$B_L = \frac{B_d}{\delta^2} = \frac{\rho g L^2}{T}. \tag{3.6}$$

The scaled system can be obtained by direct substitution into (2.1), (2.2), (2.5)–(2.8) and (2.13)–(2.16).

4. Basic state

We consider a steady, unidirectional, fully developed flow down the plate in the X-direction; see Towell & Rothfeld (1966), Allen & Biggin (1974). Under these assumptions the rivulet flow satisfies

$$\bar{U}_{YY} + \delta^2 \bar{U}_{ZZ} = -1, \tag{4.1a}$$

$$\bar{P}_Y = \bar{P}_Z = 0, \tag{4.1b, c}$$

$$-\bar{P} = \frac{\delta^2}{B_d} H_{ZZ} (1 + \delta^2 H_Z^2)^{-\frac{3}{2}} \quad \text{on } Y = H, \tag{4.2}$$

$$\bar{U}_Y - \delta^2 \bar{U}_Z H_Z = 0 \quad \text{on } Y = H, \tag{4.3}$$

$$\bar{U} = \frac{\kappa}{H} \bar{U}_Y \quad \text{on } Y = 0. \tag{4.4}$$

Since the fluid wets the solid on a strip of constant width

$$-1 \leqslant Z \leqslant 1, \tag{4.5}$$

and since all flow quantities are X-independent, we have conditions at the contact line:

$$H = 0 \quad \text{at } Z = \pm 1, \tag{4.6}$$

$$\delta H_Z = \mp \tan\phi \quad \text{at } Z = \pm 1. \tag{4.7}$$

Consistent with the definition of d, we pose the normalization condition

$$H = 1 \quad \text{at } Z = 0. \tag{4.8}$$

From (4.1*b*, *c*) we conclude that the pressure is a constant and thus (4.2) tells us that the interface forms a cylindrical meniscus whose cross-section is the arc of a circle. We shall seek approximations to $\bar{U}(Y, Z)$ and $H(Z)$ for the case of shallow, wide rivulets, i.e. $\delta \ll 1$. Assuming that $\delta^2/B_d = 1/B_L = O(1)$ as $\delta \to 0$, Weiland & Davis (1981) find that

$$\bar{U} = [H_0\, Y - \tfrac{1}{2}Y^2 + \kappa] + \delta^2[\tfrac{1}{3}Y^2 + Y(-H_0^2 + 5Z^2H_0) + \kappa(-H_0 + 4Z^2)] + O(\delta^4), \quad (4.9a)$$

$$H = H_0 + \delta^2 Z^2 H_0^2 + O(\delta^4), \quad (4.9b)$$

$$\bar{P} = B_L^{-1}(2 - 2\delta^2) + O(\delta^4), \quad (4.9c)$$

$$\phi = \delta(2 + \tfrac{4}{3}\delta^2) + O(\delta^5), \quad (4.9d)$$

where

$$H_0 = 1 - Z^2. \quad (4.9e)$$

The terms proportional to κ in (4.9*a*) should really be discarded since they arise from our allowance of slip along the rivulet. See the footnote on p. 4.

We note that $\delta \to 0$ is formally a singular perturbation of (4.1*a*). However, forms (4.9) do satisfy all the boundary conditions and the expansions are uniformly valid on the domain $-1 \leqslant Z \leqslant 1$. Thus, a uniformly valid approximation is obtained by only using the 'outer' solution. This circumstance, a common occurrence when using lubrication theory, has been clarified by Young & Davis (1985).

5. Linear theory: general

We disturb the basic state (4.9) as follows:

$$(U, V, W, P, h, A, B) = (\bar{U}, 0, 0, \bar{P}, H, 1, 1) + (u', v', w', p', h', A', B'), \quad (5.1)$$

substitute these into the scaled version of the governing system of §2 and linearize in primed quantities. For each dependent variable ψ' we introduce normal modes as follows:

$$\psi'(X, Y, Z, T) = \psi(Y, Z)\, e^{i(X - cT)}, \quad (5.2)$$

where the complex wave speed c,

$$c = c_R + ic_I, \quad (5.3)$$

determines the stability characteristics of the basic state. The governing normal-mode system is as follows:

$$kR[i(\bar{U} - c) + \bar{U}_Y v + \bar{U}_Z w] = -ip - k^2 u + u_{YY} + \delta^2 u_{ZZ}, \quad (5.4a)$$

$$ik^3 R(\bar{U} - c)\, v = -p_Y + k^2\{-k^2 v + v_{YY} + \delta^2 v_{ZZ}\}, \quad (5.4b)$$

$$ik^3 R(\bar{U} - c)\, w = -\delta^2 D p_Z + k^2\{-k^2 w + w_{YY} + \delta^2 w_{ZZ}\}, \quad (5.4c)$$

$$iu + v_Y + w_Z = 0, \quad (5.4d)$$

subject to boundary conditions on the interface

$$v = i(\bar{U} - c)\, h + wH_Z \quad \text{on } Y = H, \quad (5.4e)$$

$$-p + 2k^2\{v_Y + \delta^2 w_Z H_Z^2 - H_Z[\delta^2 v_Z + w_Y]\} N^{-2} = k\left\{\frac{-k^2}{B_d} h N^{-1} + \frac{1}{B_L}[N^{-3} h_Z]_Z\right\} \quad \text{on } Y = H, \quad (5.4f)$$

$$2\delta^2 H_Z^2 [v_Y - w_Z] - i\delta^2 h[\bar{U}_Y H_Z + \bar{U}_Z] + (1 - \delta^2 H_Z^2)[\delta^2 v_Z + w_Y] = 0 \quad \text{on } Y = H, \quad (5.4g)$$

$$u_Y + ik^2 v - H_Z[\delta^2 u_Z + ik^2 w] - \delta^2 \bar{U}_Z h_Z + h[\bar{U}_{YY} - \delta^2 H_Z \bar{U}_{ZY}] = 0 \quad \text{on } Y = H, \quad (5.4h)$$

and conditions on the solid

$$u = \frac{\kappa}{H}\left[u_Y - \frac{h}{H}\bar{U}_Y\right] \quad \text{on } Y = 0, \tag{5.4i}$$

$$v = 0 \qquad \text{on } Y = 0, \tag{5.4j}$$

$$w = \frac{\kappa}{H} w_Y \qquad \text{on } Y = 0, \tag{5.4k}$$

and conditions at the contact lines:

(1) Contact condition

$$h + H_Z A = 0, \quad Z = 1,$$

$$h - H_Z B = 0, \quad Z = -1, \tag{5.4l}$$

(2) Contact-angle-varies-with-speed condition

$$\frac{\delta^2}{U_s G'(0)}\left[h_Z - \frac{H_{ZZ}}{H_Z} h\right] = -ikN^2 c \frac{h}{H_Z}, \quad Z = \pm 1, \tag{5.4m}$$

where

$$N = (1 + \delta^2 H_Z^2)^{\frac{1}{2}}. \tag{5.4n}$$

(3) Bounded-velocity condition.

The scaled system (5.4) contains the two small parameters k and δ. In order to use an asymptotic method for analysis of this system we determine the order of δ with respect to k. First of all, note that if $\delta = 0$, then the dimensional width $L = \infty$, say, so that we have a rivulet which is infinitely wide in the cross-stream direction, i.e. a film flow. There are no contact lines, the edge conditions there are lost. Since we scale the dimensional cross-stream coordinate z on L, the limit $\delta \to 0$ in system (5.4) is a singular perturbation. Thus, we restrict taking this limit in any results we obtain. In contrast to Weiland & Davis (1981) we shall pose the class of problems such that

$$\delta^2 = Dk^s, \tag{5.5a}$$

where D is a constant,

$$D = O(1), \tag{5.5b}$$

and $s > 0$. We take $s \neq 0$, so that we can simplify the system to ordinary differential equations for the velocity components.

After choosing the value of s we then consider the effects of surface tension. From the normal stress boundary condition (5.4f) we see that the dominant surface tension terms are

$$\frac{k^2}{B_d} h, \tag{5.6a}$$

and

$$\frac{1}{B_L} h_{ZZ} \equiv \frac{\delta^2}{B_d} h_{ZZ}, \tag{5.6b}$$

where the former gives a measure of longitudinal curvature effects while the latter gives transverse curvature effects. Clearly, from relations (5.6) when $0 < s < 2$,

$$\frac{1}{B_L} \gg \frac{k^2}{B_d}, \tag{5.7}$$

and when $s > 2$,

$$\frac{k^2}{B_d} \gg \frac{1}{B_L}. \tag{5.8}$$

The two effects balance when $s = 2$. Therefore, in order to retain the appropriate surface tension effect, we take

$$\frac{1}{B_L} = O(1) \quad (0 < s < 2), \tag{5.9a}$$

and

$$\frac{k^2}{B_d} \equiv \frac{1}{\bar{B}_d} = O(1) \quad (s \geqslant 2). \tag{5.9b}$$

This is reasonable from a physical standpoint since the Bond number B_d is small ($B_d \approx 0.14$ for a water rivulet with a height of 1 mm). Krantz & Goren (1970) retain these terms (5.9*b*) in their film flow analysis while Weiland & Davis (1981) use (5.9*a*) in their analysis.

We shall now discuss the case $s = \frac{1}{2}$ in detail. In §8 we discuss the results for larger values of s.

6. Linear theory: 'narrow' rivulets with $s = \frac{1}{2}$

We set $s = \frac{1}{2}$ and write for each dependent variable ψ and for complex eigenvalue c,

$$\left.\begin{aligned} \psi &= \psi_0 + k^{\frac{1}{2}}\psi_1 + k\psi_2 + O(k^{\frac{3}{2}}), \\ c &= c_0 + k^{\frac{1}{2}}c_1 + kc_2 + O(k^{\frac{3}{2}}). \end{aligned}\right\} \tag{6.1}$$

The basic state (4.9) is known in powers of δ^2 so that we also have

$$\left.\begin{aligned} \bar{U} &= \bar{U}_0 + Dk^{\frac{1}{2}}\bar{U}_1 + O(D^2k), \\ H &= H_0 + Dk^{\frac{1}{2}}H_1 + O(D^2k). \end{aligned}\right\} \tag{6.2}$$

When forms (6.1) and (6.2) are substituted into system (5.4), we obtain at order unity:

$$u_{0YY} - \mathrm{i}p_0 = 0, \tag{6.3a}$$

$$p_{0Y} = 0, \tag{6.3b}$$

$$Dp_{0Z} = 0, \tag{6.3c}$$

$$\mathrm{i}u_0 + v_{0Y} + w_{0Z} = 0 \tag{6.3d}$$

$$v_0 = -\mathrm{i}(u_0 - c_0) + w_0 H_{0Z} \quad (Y = H_0), \tag{6.3e}$$

$$-p_0 = 0 \quad (Y = H_0), \tag{6.3f}$$

$$w_{0Y} = 0 \quad (Y = H_0), \tag{6.3g}$$

$$u_{0Y} + h_0 \bar{U}_{0YY} = 0 \quad (Y = H_0), \tag{6.3h}$$

$$u_0 = \frac{\kappa}{H_0}\left[u_{0Y} - \frac{H_0}{H_{0Z}}\bar{U}_{0Y}\right] \quad (Y = 0), \tag{6.3i}$$

$$v_0 = 0 \quad (Y = 0), \tag{6.3j}$$

$$w_0 = \frac{\kappa}{H_0}w_{0Y} \quad (Y = 0), \tag{6.3k}$$

with contact-line conditions

$$h_0 + H_{0Z} A_0 = 0 \quad (Z = 1), \tag{6.4a}$$

$$h_0 - H_{0Z} B_0 = 0 \quad (Z = -1), \tag{6.4b}$$

$$h_{0Z} - \frac{H_{0ZZ}}{H_{0Z}} h_0 = 0 \quad (Z = \pm 1). \tag{6.4c}$$

At order $k^{\frac{1}{2}}$ we have

$$u_{1YY} - \mathrm{i}p_1 = -Du_{0ZZ}, \tag{6.5a}$$

$$p_{1Y} = 0, \tag{6.5b}$$

$$Dp_{1Z} = 0, \tag{6.5c}$$

$$\mathrm{i}u_1 + v_{1Y} + w_{1Z} = 0, \tag{6.5d}$$

$$v_1 + Dv_{0Y} H_1 = -\mathrm{i}c_1 h_0 - \mathrm{i}(\bar{U}_0 - c_0) h_1 + \mathrm{i}D\bar{U}_1 h_0 + w_1 H_{0Z} + Dw_0 H_{1Z} + \mathrm{i}\bar{U}_{0Y} DH_1 h_0 + Dw_{0Y} H_1 H_{0Z} \quad (Y = H_0), \tag{6.5e}$$

$$-p_1 = 0 \quad (Y = H_0), \tag{6.5f}$$

$$2DH_{0Z}[v_{0Y} - w_{0Z}] - \mathrm{i}Dh_0[\bar{U}_{0Y} H_{0Z} + \bar{U}_{0Z}] + w_{1Y} + w_{0YY} DH_1 - DH_{0Z}^2 w_{0Y} + Dv_{0Z} = 0 \quad (Y = H_0), \tag{6.5g}$$

$$u_{1Y} + u_{0YY} DH_1 - DH_{0Z} u_{0Z} - Dh_{0Z} \bar{U}_{0Z} + h_1 \bar{U}_{0YY} + h_0 D\bar{U}_{1YY} + h_0 \bar{U}_{0YYY} DH_1 - Dh_0 H_{0Z} \bar{U}_{0ZY} = 0 \quad (Y = H_0), \tag{6.5h}$$

$$u_1 = \frac{\kappa}{H_0}\left[u_{1Y} - \frac{h_0}{H_0} D\bar{U}_{1Y} - \frac{h_1}{H_0}\bar{U}_{0Y} + \frac{h_0}{H_0^2} DH_1 \bar{U}_{0Y}\right] - \frac{\kappa}{H_0^2} DH_1 \left[u_{0Y} - \frac{h_0}{H_0}\bar{U}_{0Y}\right] \quad (Y = 0), \tag{6.5i}$$

$$v_1 = 0 \quad (Y = 0), \tag{6.5j}$$

$$w_1 = \frac{\kappa}{H_0} w_{1Y} - \frac{\kappa}{H_0^2} DH_1 w_{0Y} \quad (Y = 0), \tag{6.5k}$$

with contact-line conditions

$$h_1 + H_{0Z} A_1 + DH_{1Z} A_0 = 0 \quad (Z = 1), \tag{6.6a}$$

$$h_1 - H_{0Z} B_1 - DH_{1Z} B_0 = 0 \quad (Z = -1), \tag{6.6b}$$

$$\frac{D}{U_s G'(0)}\left[h_{1Z} - \frac{H_{0ZZ} h_1}{H_{0Z}} - \frac{DH_{1ZZ} h_0}{H_{0Z}} + \frac{H_{0ZZ}}{H_{0Z}^2} DH_{1Z} h_0\right] = \frac{-\mathrm{i}c_0 h_0}{H_{0Z}} \quad (Z = \pm 1). \tag{6.6c}$$

We shall need only some of the equations at orders k, $k^{\frac{3}{2}}$, and k^2. At order k these are

$$u_{2YY} - \mathrm{i}p_2 + Du_{1ZZ} = R[-\mathrm{i}(\bar{U}_0 - c_0) u_0 + \bar{U}_{0Y} v_0 + \bar{U}_{0Z} w_0], \tag{6.7a}$$

$$p_{2Y} = 0, \tag{6.7b}$$

$$Dp_{2Z} = 0, \tag{6.7c}$$

$$-p_2 = \frac{1}{B_L} h_{0ZZ} \quad (Y = H_0), \tag{6.7d}$$

$$u_{2Y}+u_{1YY}\,DH_1+u_{0YY}\,D^2H_2+\tfrac{1}{2}u_{0YYY}\,D^2H_1^2-D^2H_{1Z}\,u_{0Z}-DH_{0Z}\,u_{1Z}-D^2H_{0Z}\,u_{0ZY}\,H_1$$
$$-D^2\bar{U}_{1Z}\,h_{0Z}-D\bar{U}_{0Z}\,h_{1Z}-D^2\bar{U}_{0ZY}\,H_1\,h_{0Z}+h_2\,\bar{U}_{0YY}+Dh_1\,\bar{U}_{1YY}+D^2h_0\,\bar{U}_{2YY}$$
$$+h_1\,D\bar{U}_{0YYY}\,H_1+h_0\,D^2\bar{U}_{0YYY}\,H_2+\tfrac{1}{2}h_0\,\bar{U}_{0YYYY}\,D^2H_1^2+h_0\,D^2\bar{U}_{1YYY}\,H_1$$
$$-h_1\,DH_{0Z}\,\bar{U}_{0ZY}-h_0\,D^2H_{1Z}\,\bar{U}_{0ZY}-h_0\,D^2H_{0Z}\,\bar{U}_{1ZY}-h_0\,D^2H_{0Z}\,\bar{U}_{0ZYY}\,H_1=0$$
$$(Y=H_0), \quad (6.7e)$$

$$u_2=\frac{\kappa}{H_0}\Big[u_{2Y}-\frac{h_0}{H_0}D^2\bar{U}_{2YY}-\frac{h_1\,D\bar{U}_{1Y}}{H_0}+\frac{h_0\,D^2H_1\,\bar{U}_{1Y}}{H_0}+\frac{h_0\,D^2H_2\,\bar{U}_{0Y}}{H_0^2}$$
$$-\frac{h_2\,\bar{U}_{0Y}}{H_0}+\frac{h_1\,DH_1\,\bar{U}_{0Y}}{H_0^2}-\frac{h_0\,D^2H_1^2\,\bar{U}_{0Y}}{H_0^3}\Big]+\Big[\frac{-\kappa D^2H_2}{H_0^2}+\frac{\kappa D^2H_1^2}{H_0^3}\Big]\Big[u_{0Y}-\frac{h_0}{H_0}\bar{U}_{0Y}\Big]$$
$$-\frac{\kappa}{H_0^2}DH_1\Big[u_{1Y}-\frac{h_0}{H_1}D\bar{U}_{1Y}-\frac{h_1}{H_0}\bar{U}_{0Y}+\frac{h_0}{H_1}DH_0\,\bar{U}_{0Y}\Big] \quad (Y=0), \quad (6.7f)$$

with contact-line conditions

$$h_2+H_{0Z}\,A_2+DH_{1Z}\,A_1+D^2H_{2Z}\,A_0=0 \quad (Z=1), \quad (6.8a)$$
$$h_2-H_{0Z}\,B_2-DH_{1Z}\,B_1-D^2H_{2Z}\,B_0=0 \quad (Z=-1), \quad (6.8b)$$
$$\frac{D}{U_S\,G'(0)}\Big[h_{2Z}-\frac{H_{0ZZ}\,h_2}{H_{0Z}}-\frac{DH_{1ZZ}\,h_1}{H_{0Z}}+\frac{DH_{0ZZ}\,H_{1Z}\,h_1}{H_{0Z}^2}-\frac{D^2H_{2ZZ}\,h_0}{H_{0Z}}$$
$$+\frac{D^2H_{1ZZ}\,H_{1Z}\,h_0}{H_{0Z}^2}+\frac{D^2H_{0ZZ}\,H_{2ZZ}\,h_0}{H_{0Z}^2}-\frac{D^2H_{0ZZ}\,H_{1Z}^2\,h_0}{H_{0Z}^3}\Big]$$
$$=-\mathrm{i}c_1\frac{h_0}{H_{0Z}}-\frac{\mathrm{i}c_0\,h_1}{H_{0Z}}+\frac{\mathrm{i}c_0\,h_0\,DH_{1Z}}{H_{0Z}^2}-\mathrm{i}c_0\,h_0\,DH_{0Z} \quad (Z=\pm1). \quad (6.8c)$$

In writing down (6.7*d*) we have assumed, as discussed above, that

$$\frac{\delta^2}{B_d}=\frac{Dk^{\frac{1}{2}}}{B_d}=\frac{1}{B_L}, \quad (6.9)$$

and

$$\frac{1}{B_L}=O(1) \quad \text{as } k\to0. \quad (6.10)$$

At order $k^{\frac{3}{2}}$ we use

$$p_{3Y}=0, \quad (6.11a)$$
$$-Dp_{3Z}+w_{0YY}=0, \quad (6.11b)$$
$$-p_3=\frac{1}{B_L}h_{1ZZ}-\frac{3}{2}\frac{1}{B_L}D[h_{0Z}\,H_{0Z}^2]_Z \quad (Y=H_0). \quad (6.11c)$$

And finally at order k^2 we use

$$-p_{4Y}+v_{0YY}=0, \quad (6.12a)$$
$$-Dp_{4Z}+w_{1YY}+Dw_{0ZZ}=0, \quad (6.12b)$$
$$-p_4+2[v_{0Y}-H_{0Z}\,w_{0Y}]=\frac{1}{B_L}h_{2ZZ}-\frac{3}{2}\frac{1}{B_L}D[h_{1Z}\,H_{0Z}^2]_Z$$
$$-3\frac{1}{B_L}D^2[h_{0Z}\,H_{0Z}\,H_{1Z}]_Z+\frac{15}{8}\frac{1}{B_L}D^2[h_{0Z}\,H_{0Z}^4]_Z \quad (Y=H_0). \quad (6.12c)$$

The above system of equations are nearly identical to those in Weiland & Davis (1981). The difference is that we retain the kinematic condition in the pointwise forms (6.3*e*) and (6.5*e*). This is essential to completing the analysis.

6.1. *Fixed contact lines*

The contact lines become fixed when $G'(0)\to\infty$ as seen from relation (5.4*m*) since

$$h = 0 \quad \text{at } Z = \pm 1, \tag{6.13}$$

which gives from relation (5.4*l*) that

$$A = B = 0. \tag{6.14}$$

Since the contact lines are stationary, we can set the slip coefficient $\kappa = 0$.

Given that linear stability theory represents a homogeneous eigenvalue problem, we pose a normalization condition, namely

$$h = 1 \quad \text{at } Z = 0, \tag{6.15}$$

which determines the arbitrary multiplicative constant associated with the eigenfunction.

To solve this system we consider (6.3*b*, *c*, *f*) and find that

$$p_0 = 0. \tag{6.16}$$

Similarly, (6.5*b*, *c*, *f*) give

$$p_1 = 0. \tag{6.17}$$

Again, (6.7*b*, *c*) give that p_2 is constant; (6.7*d*) and (6.13) then give that

$$h_0 = \tfrac{1}{2}B_L\, p_2[1-Z^2], \tag{6.18}$$

and using the normalization condition (6.15) we find that

$$p_2 = 2B_L^{-1} \tag{6.19}$$

and

$$h_0 = 1-Z^2. \tag{6.20}$$

The streamwise velocity u_0 is then obtained from (6.3*a*) subject to conditions (6.3*h*) and (6.3*i*). We find that

$$u_0 = h_0\, Y. \tag{6.21}$$

Next, since (6.11*a*) gives p_3 independent of Y, then p_3 is given for all Y by (6.11*c*). However, at this point h_1 is still unknown. In order to determine h_1 we first obtain the transverse velocity w_0 from (6.11*b*) subject to conditions (6.3*g*) and (6.3*k*):

$$w_0 = Dp_{3Z}\, Y(\tfrac{1}{2}Y-H_0). \tag{6.22}$$

Then, using (6.3*d*) and (6.3*j*), we solve for v_0 to obtain

$$v_0 = -\tfrac{1}{2}\mathrm{i}h_0\, Y^2-\tfrac{1}{6}Dp_{3ZZ}\, Y^3+\tfrac{1}{2}Dp_{3ZZ}\, Y^2H_0+\tfrac{1}{2}Dp_{3Z}\, Y^2H_{0Z}. \tag{6.23}$$

We now substitute (6.21), (6.22) and (6.23) into the kinematic condition (6.3*e*) and rewrite in terms of p_3 to obtain:

$$[\tfrac{1}{3}Dp_{3Z}\, H_0^3]_Z = \mathrm{i}(H_0^2-c_0)\, h_0. \tag{6.24}$$

Now, since p_3 is proportional to h_{1ZZ} by relation (6.11*c*), then (6.24) is a non-homogeneous fourth-order differential equation for h_1 in the transverse variable Z. The general solution will contain four integration constants plus the unknown

eigenvalue c_0. Thus we need five boundary conditions. Three of them are given by (6.13) and (6.15). The other two come from the bounded-velocity condition. If we integrate (6.24) and substitute for p_{3Z} in (6.22), we find that the condition of bounded velocity at the contact lines $Z = \pm 1$ requires that the constant of integration be set equal to zero; this determines c_0,

$$c_0 = \tfrac{24}{35} = 0.686. \tag{6.25}$$

c_0 is the phase speed of the small-amplitude waves and its magnitude is twice the average surface speed of the basic-state rivulet (Weiland & Davis 1981).

This agrees with the result of Weiland & Davis (1981) who require only a satisfaction of the kinematic condition in integrated form. However, Weiland & Davis are unable to determine h_1 since the kinematic condition is not applied pointwise.

We solve (6.24) using (6.13) and (6.15) to obtain

$$\begin{aligned} h_1 = {} & 3DZ^2(1-Z^2) - \mathrm{i}D^{-1}B_L Z^2[0.339 + \tfrac{1}{56}Z^2] + \mathrm{i}D^{-1}B_L \\ & \times\{-0.129(1-Z^2)\log(1-Z^2) + 0.257\,[(1+Z)\log(1+Z) + (1-Z)\log(1-Z)]\}. \end{aligned} \tag{6.26}$$

The procedure to determine the eigenvalue corrections follows similarly. We see that (6.12*a*) subject to condition (6.12*c*) allows us to determine p_4 in terms of the unknown h_2. We solve for the velocity components u_1, v_1, and w_1, and substitute them into the kinematic condition (6.5*e*). As before, this results in a fourth-order differential equation in the transverse variable Z. The boundary conditions are (6.13), (6.15) and the bounded-velocity condition. Upon integration of this equation and the requiring of bounded velocities, we obtain the eigenvalue correction

$$c_1 = c_{1\mathrm{R}} + \mathrm{i}c_{1\mathrm{I}} = -0.538D - 0.0033\mathrm{i}D^{-1}B_L. \tag{6.27}$$

Stability is determined through the sign of c_{I}. At this point we have only the leading-order term $c_{1\mathrm{I}}$ and this contains no kinematic terms. From (6.7*a*) we see that we need to go to order k in order to get them. The algebra becomes very complicated at this order. Since we only want the correction $c_{2\mathrm{I}}$, we shall simplify matters as follows. First of all, rather than determining u_2, v_2, and w_2, and then using the kinematic condition to obtain a differential equation for h_3, which we would integrate once and apply the bounded-velocity condition to obtain c_2, we shall use a method based upon (2.17). The order-k form, obtained by integrating (2.17) with respect to Z, linearizing, and then evaluating the resulting expression at the contact lines gives the mass flux through the contact line as follows:

$$\begin{aligned} \int_0^{H_0} w_2\,\mathrm{d}Y = -\mathrm{i}\Big\{ \int [& D^2\bar{U}_2(H_0,\pm1)h_0 + D^2\bar{U}_{1Y}(H_0,\pm1)H_1h_0 + D\bar{U}_1(H_0,\pm1)h_1 \\ & + \tfrac{1}{2}D^2\bar{U}_{0YY}(H_0,\pm1)H_1^2h_0 + D^2\bar{U}_{0Y}(H_0,\pm1)H_2h_0 + D\bar{U}_{0Y}(H_0,\pm1)H_1h_1 \\ & + \bar{U}_0(H_0,\pm1)h_2 - c_2h_0 - c_1h_1 - c_0h_2]\,\mathrm{d}Z + \int\Big[D^2u_0(H_0,\pm1)H_2 \\ & + Du_1(H_0,\pm1)H_1 + \tfrac{1}{2}D^2u_{0Y}(H_0,\pm1)H_1^2 + \int_0^{H_0} u_2\,\mathrm{d}Y\Big]\mathrm{d}Z\Big\} + b, \end{aligned} \tag{6.28}$$

where b is a constant of integration. If the velocity is bounded, then the mass-flux vanishes and the right-hand side of (6.28) must be zero. The resulting equation has four unknowns, u_2, h_2, c_2, and b. However, we can solve for u_2 and h_2 from previous work and thus, since form (6.28) applies at both $Z = \pm 1$, we have two equations to

determine the two unknowns c_2 and b. To make matters even simpler, we solve only for $c_{2\mathrm{I}}$ and thus need only to determine the imaginary parts of u_2 and h_2. Using this simplification, we solve for $c_{2\mathrm{I}}$ and $\mathrm{Im}(b)$ from the following two equations obtained from (6.28):

$$\int\Big[D\bar{U}_1(H_0,\pm1)\,\mathrm{Im}(h_1)+\bar{U}_0(H_0,\pm1)\,\mathrm{Im}(h_2)-c_{2\mathrm{I}}h_0-\mathrm{Im}(c_1h_1)$$

$$-c_0\,\mathrm{Im}(h_2)+DH_0H_1\,\mathrm{Im}(h_1)+\int_0^{H_0}\mathrm{Im}(u_2)\,\mathrm{d}Y\Big]\mathrm{d}Z+\mathrm{Im}(b)=0. \quad (6.29)$$

To get $\mathrm{Im}(h_2)$ we solve the fourth-order differential equation for h_2 using the contact-line conditions (6.13), 6.15) and bounded velocities. Then, to get $\mathrm{Im}(u_2)$, we solve (6.7a) subject to conditions (6.7e) and (6.7f). We then substitute these into (6.29) together with all the other known quantities and find that $\mathrm{Im}(b)=0$ and

$$c_{2\mathrm{I}}=0.031[R-14.7B_L^{-1}+0.483B_L]. \quad (6.30)$$

In summary, for the case of fixed, straight contact lines and

$$\delta^2=Dk^{\frac{1}{2}}, \quad (6.31)$$

we have the phase speed for linearized waves

$$c_{\mathrm{R}}=0.686-0.538Dk^{\frac{1}{2}}+O(k). \quad (6.32)$$

These flat rivulets on vertical walls are stable to small, long-wave disturbances as long as $c_{\mathrm{I}}<0$, where

$$c_{\mathrm{I}}=-k^{\frac{1}{2}}0.0033B_L\,D^{-1}+0.031k[R-14.7B_L^{-1}+0.483B_L]+O(k^{\frac{3}{2}}). \quad (6.33)$$

We note here that the term proportional to B_L^{-1} in relation (6.33) represents the same surface-tension mechanism which stabilizes two-dimensional long waves in film flow. However, we see that the presence of the fixed contact lines adds an additional stabilizing mechanism proportional to $B_L=B_d/Dk^{\frac{1}{2}}$. Thus its effects are strongly felt when surface tension is small.

6.2. *Moving contact lines*

For the case of moving contact lines let us consider the contact line condition (5.4m) in the form

$$h_Z-\frac{H_{ZZ}h}{H_Z}=-\mathrm{i}cG_1\frac{h}{H_Z}(1+\delta^2H_Z^2)\quad(Z=\pm1), \quad (6.34)$$

where

$$G_1=\frac{kU_{\mathrm{s}}G'(0)}{\delta^2}. \quad (6.35)$$

We shall assume that G_1 is an order unity parameter so that we can use the full contact-angle-versus-speed condition (6.34). Then by varying G_1 through the range

$$0\leqslant G_1<\infty, \quad (6.36)$$

which is equivalent to letting $G'(0)$ vary from 0 to ∞, we shall be able to describe the contact-line motion from a fixed contact angle to a fixed contact-line regime. This of course will be done by keeping δ^2 fixed. However, it is noted that one could also vary G_1 as in range (6.36) by letting δ^2 vary from ∞ to 0. According to (3.2), this means that the rivulet becomes wider. In other words even though the contact

lines can move, the rivulet can be so wide that these effects are overwhelmed and the overall result is similar to that of a fixed contact-line case. That such an explanation is reasonable will become more apparent when we show that fixed-contact-line-rivulet behaviour appears to be the same as that of a film flow.

The governing equations, boundary conditions, and normalization conditions for moving contact lines are those given in (6.3)–(6.12) and (6.15), except for conditions (6.4*c*), (6.6*c*), and (6.8*c*). At orders 1, $k^{\frac{1}{2}}$, and k these, respectively, become

$$h_{0Z}-\frac{H_{0ZZ}h_0}{H_{0Z}}=-ic_0G_1\frac{h_0}{H_{0Z}}\quad(Z=\pm1), \tag{6.37}$$

$$h_{1Z}-\frac{H_{0ZZ}h_1}{H_{0Z}}-\frac{DH_{1ZZ}h_0}{H_{0Z}}+\frac{H_{0ZZ}DH_{1Z}h_0}{H_{0Z}^2}$$
$$=iG_1\left[\frac{-c_1h_0}{H_{0Z}}-\frac{c_0h_1}{H_{0Z}}+\frac{c_0h_0DH_{1Z}}{H_{0Z}^2}-c_0h_0DH_{0Z}\right]\quad(Z=\pm1), \tag{6.38}$$

$$h_{2Z}-\frac{H_{0ZZ}h_2}{H_{0Z}}-\frac{DH_{1ZZ}h_1}{H_{0Z}}+\frac{DH_{0ZZ}H_{1Z}h_1}{H_{0Z}^2}-\frac{D^2H_{2ZZ}h_0}{H_{0Z}}+\frac{D^2H_{1ZZ}H_{1Z}h_0}{H_{0Z}^2}$$
$$+\frac{D^2H_{0ZZ}H_{2ZZ}h_0}{H_{0Z}^2}-\frac{D^2H_{0ZZ}H_{1Z}^2h_0}{H_{0Z}^3}$$
$$=-iG_1\left[\frac{c_2h_0}{H_{0Z}}+\frac{c_1h_1}{H_{0Z}}-\frac{c_1h_0DH_{1Z}}{H_{0Z}^2}+\frac{c_0h_2}{H_{0Z}}-\frac{c_0h_1DH_{1Z}}{H_{0Z}^2}-\frac{c_0h_0D^2H_{2Z}}{H_{0Z}^2}\right.$$
$$\left.+\frac{c_0h_0D^2H_{1Z}^2}{H_{0Z}^3}+c_1h_0DH_{0Z}+c_0h_1DH_{0Z}+2c_0h_0DH_{1Z}\right]\quad(Z=\pm1). \tag{6.39}$$

We now proceed exactly as before and again we find

$$p_0=p_1=0. \tag{6.40}$$

Next, (6.7*b*, *c*) give that p_2 is a constant. We then determine the leading-order boundary perturbation h_0 from conditions (6.7*d*) and (6.41). We find, using the normalization condition (6.15), that

$$h_0=1-SZ^2, \tag{6.41}$$

where

$$S=\frac{1+\frac{1}{2}ic_0G_1}{-1+\frac{1}{2}ic_0G_1}, \tag{6.42}$$

and

$$p_2=\frac{2S}{B_L}. \tag{6.43}$$

Note that as $G_1\to\infty$, then $S\to1$ so that

$$h_0=1-Z^2, \tag{6.44}$$

and $p_2>0$ for fixed contact lines, and that as $G_1\to0$, $S\to-1$ so that

$$h_0=1+Z^2, \tag{6.45}$$

and $p_2<0$ for fixed contact angles. This result is similar to that of Weiland & Davis (1981) except that they have an additional term a_0Z in their fixed contact angle result, where a_0 is an arbitrary constant. We too would get this result if we set $G_1\equiv0$ in form (6.34). However, further analysis will show that we need $a_0\equiv0$ in order to

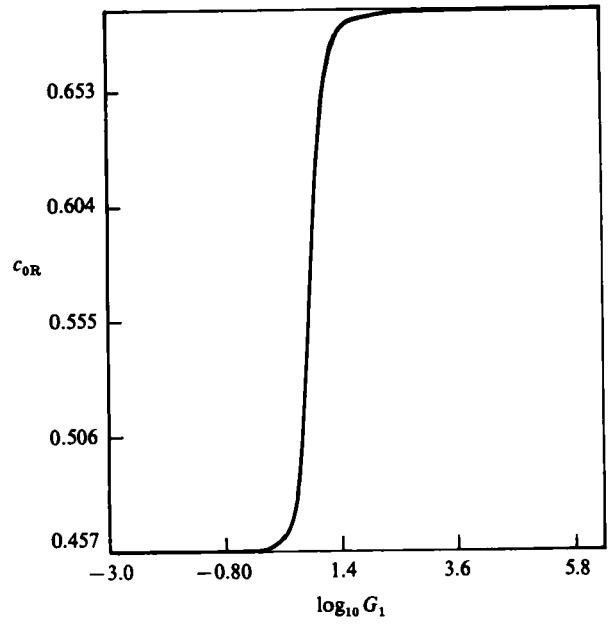

FIGURE 2. The phase speed c_{0R} of the long-wave disturbances is plotted versus G_1 for various values of the slip coefficient ($\kappa = 10^{-8}, 10^{-3}$). The curves are indistinguishable.

satisfy the bounded-velocity condition. In addition we have extended the results of Weiland & Davis (1981) in (6.41) to describe the interface behaviour as the contact-line motion varies from fixed contact angle to fixed contact-lines.

The contact condition (6.4a) implies that the contact-line correction for each case is

$$\left.\begin{aligned} G_1 \to \infty: \quad A_0 &= \frac{-h_0}{H_{0Z}} = 0 \quad \text{at } Z = 1, \\ G_1 \to 0: \quad A_0 &= \frac{-h_0}{H_{0Z}} = 1 \quad \text{at } Z = 1. \end{aligned}\right\} \tag{6.46}$$

In other words the contact lines are most mobile for the case of fixed contact angle and spread more slowly and through smaller distances as $G_1 \to \infty$. This is consistent with our defining $G'(0)$ as a quantity that measures the ability of a contact line to spread for a given liquid–solid system.

The streamwise velocity u_0 is now obtained from (6.3a) subject to conditions (6.3h) and (6.3i). The slip coefficient κ is taken different from zero for this case since contact-line motion occurs. This follows our discussion of the no slip condition in §2. Independent of the value of κ, we still find

$$u_0 = h_0\, Y. \tag{6.47}$$

Next, as before, p_3 is given exactly by condition (6.11c) and h_1 is still unknown. So we determine the transverse velocity w_0 from (6.11b) subject to conditions (6.3g) and (6.3k). We obtain

$$w_0 = Dp_{3Z}(\tfrac{1}{2}Y^2 - H_0\, Y - \kappa). \tag{6.48}$$

Then, using conditions (6.3d) and (6.3j), we solve for v_0 and find

$$v_0 = -\tfrac{1}{2}ih_0\, Y^2 - \tfrac{1}{6}Dp_{3ZZ}\, Y^3 + \tfrac{1}{2}Dp_{3ZZ}\, Y^2 H_0 + \tfrac{1}{2}Dp_{3Z}\, Y^2 H_{0Z} + \kappa Dp_{3ZZ}\, Y. \tag{6.49}$$

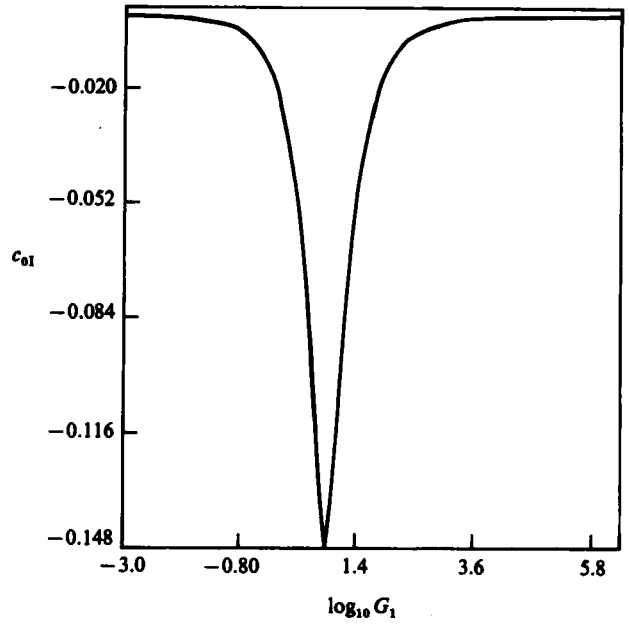

FIGURE 3. The coefficient c_{0I} is plotted versus G_1 for various values of the slip coefficient ($\kappa = 10^{-8}, 10^{-3}$). The curves are indistinguishable.

We now substitute forms (6.47), (6.48), and (6.49) into the kinematic condition (6.3*e*). As before, this results in a fourth-order differential equation in the transverse variable Z for h_1. We have

$$[\tfrac{1}{3}Dp_{3Z}H_0^3+\kappa Dp_{3Z}H_0]_Z = \mathrm{i}[-c_0 h_0+h_0 H_0^2], \tag{6.50}$$

where p_3 is proportional to h_{1ZZ}. This time the four integration constants and unknown eigenvalue c_0 are determined through the normalization condition (6.15), the moving-contact-line conditions (6.38) and the bounded-velocity condition. After one integration of (6.50) we apply the boundedness condition to (6.48) and determine the integration constant to be zero and find the leading-order eigenvalue

$$c_0 = \frac{8(7-S)}{35(3-S)}+\kappa. \tag{6.51}$$

When $G_1 \to 0$ and thus $S \to -1$ we have

$$c_0 = \tfrac{16}{35}+\kappa = 0.457+\kappa, \tag{6.52}$$

which is the phase speed for small amplitude waves on rivulets with fixed contact angles. This result agrees with that of Weiland & Davis (1981). At the other extreme, $G_1 \to \infty$, we recover condition (6.25). Figures 2 and 3 show how c_{0R} and c_{0I} vary with G_1 and table 1 gives numerical values. Either from the table or from substituting S into relation (6.51) and solving for c_0, one sees that† c_{0I} varies as G_1 for small G_1 and as $1/G_1$ for large G_1. In addition it is negative for all G_1. Thus the contact-angle-increasing-with-contact-line-speed effect is always stabilizing to the system. This too agrees with earlier findings of Davis (1980).

We note that the form of (6.51) and the value of c_{0R} in table 1 suggest that we

† The second root of the quadratic equation gives a strongly damped mode.

(a)

G_1	c_{0R}	c_{0I}	S_R	S_I	C_2	C_{2R}	C_3	C_{3R}	C_4	C_5	C_7	C_8
2.0×10^{-3}	0.457	-5.22×10^{-5}	-1.00	-9.14×10^{-4}	-1.71×10^{-1}	1.51×10^{-4}	-6.39×10^{-5}	-1.42×10^{-1}	-3.90×10^{-3}	2.29×10^{-1}	3.38×10^{-1}	1.21×10^{-3}
2.0×10^{-2}	0.457	-5.22×10^{-4}	-1.00	-9.14×10^{-3}	-1.71×10^{-1}	1.51×10^{-3}	-6.38×10^{-4}	-1.42×10^{-1}	-3.90×10^{-3}	2.29×10^{-1}	3.38×10^{-1}	1.21×10^{-2}
2.0×10^{-1}	0.457	-5.23×10^{-3}	-9.97×10^{-1}	-9.14×10^{-2}	-1.69×10^{-1}	1.49×10^{-2}	-6.27×10^{-3}	-1.41×10^{-1}	-3.85×10^{-3}	2.26×10^{-1}	3.55×10^{-1}	1.17×10^{-1}
2.0	0.464	-5.29×10^{-2}	-7.04×10^{-1}	-8.34×10^{-1}	-1.00×10^{-1}	7.01×10^{-2}	-1.06×10^{-2}	-9.05×10^{-2}	-2.02×10^{-3}	1.10×10^{-1}	6.84×10^{-1}	-1.67×10^{-1}
4.0	0.489	-1.08×10^{-1}	1.02×10^{-3}	-1.24	-6.90×10^{-2}	6.57×10^{-2}	3.97×10^{-2}	-4.81×10^{-2}	-2.37×10^{-3}	6.52×10^{-2}	6.16×10^{-1}	-3.41×10^{-1}
6.0	0.546	-1.46×10^{-1}	6.26×10^{-1}	-1.09	-5.15×10^{-2}	7.77×10^{-2}	1.30×10^{-1}	-1.71×10^{-2}	-3.79×10^{-3}	4.73×10^{-2}	1.02	-4.97×10^{-1}
7.0	0.553	-1.47×10^{-1}	6.64×10^{-1}	-1.06	-3.47×10^{-2}	8.15×10^{-2}	1.92×10^{-1}	-2.77×10^{-2}	-2.88×10^{-3}	1.36×10^{-2}	1.30	-2.27×10^{-1}
7.2	0.560	-1.48×10^{-1}	6.98×10^{-1}	-1.03	-3.12×10^{-2}	8.14×10^{-2}	2.04×10^{-1}	-3.28×10^{-2}	-2.51×10^{-3}	4.85×10^{-3}	1.33	-2.31×10^{-1}
7.4	0.566	-1.48×10^{-1}	7.27×10^{-1}	-9.96×10^{-1}	-2.78×10^{-2}	8.10×10^{-2}	2.15×10^{-1}	-3.86×10^{-2}	-2.09×10^{-3}	-4.37×10^{-3}	1.35	-1.89×10^{-1}
7.6	0.572	-1.47×10^{-1}	7.53×10^{-1}	-9.65×10^{-1}	-2.44×10^{-2}	8.03×10^{-2}	2.26×10^{-1}	-4.52×10^{-2}	-1.62×10^{-3}	-1.39×10^{-2}	1.36	-1.49×10^{-1}
7.8	0.578	-1.47×10^{-1}	7.75×10^{-1}	-9.35×10^{-1}	-2.12×10^{-2}	7.94×10^{-2}	2.36×10^{-1}	-5.23×10^{-2}	-1.12×10^{-3}	-2.37×10^{-2}	1.35	-1.12×10^{-1}
8.0	0.583	-1.46×10^{-1}	7.95×10^{-1}	-9.06×10^{-1}	-1.82×10^{-2}	7.82×10^{-2}	2.45×10^{-1}	-6.00×10^{-2}	-5.81×10^{-4}	-3.37×10^{-2}	1.34	-7.95×10^{-2}
8.2	0.588	-1.44×10^{-1}	8.12×10^{-1}	-8.78×10^{-1}	-1.53×10^{-2}	7.69×10^{-2}	2.54×10^{-1}	-6.81×10^{-2}	-1.70×10^{-4}	-4.38×10^{-2}	1.32	-5.05×10^{-2}
8.4	0.593	-1.43×10^{-1}	8.28×10^{-1}	-8.52×10^{-1}	-1.27×10^{-2}	7.55×10^{-2}	2.62×10^{-1}	-7.65×10^{-2}	5.67×10^{-4}	-5.39×10^{-2}	1.29	-2.51×10^{-2}
8.6	0.598	-1.41×10^{-1}	8.41×10^{-1}	-8.27×10^{-1}	-1.02×10^{-2}	7.40×10^{-2}	2.70×10^{-1}	-8.52×10^{-2}	1.17×10^{-3}	-6.40×10^{-2}	1.26	-3.14×10^{-3}
9.0	0.602	-1.40×10^{-1}	8.53×10^{-1}	-8.04×10^{-1}	-5.74×10^{-3}	7.06×10^{-2}	2.83×10^{-1}	-1.03×10^{-1}	2.39×10^{-3}	-8.38×10^{-2}	1.18	3.15×10^{-2}
10.0	0.632	-1.21×10^{-1}	9.22×10^{-1}	-6.23×10^{-1}	2.45×10^{-3}	6.18×10^{-2}	3.06×10^{-1}	-1.48×10^{-1}	5.40×10^{-3}	-1.31×10^{-1}	9.21×10^{-1}	7.64×10^{-2}
12.0	0.649	-1.04×10^{-1}	9.51×10^{-1}	-5.09×10^{-1}	1.01×10^{-2}	4.58×10^{-2}	3.21×10^{-1}	-2.30×10^{-1}	1.09×10^{-2}	-2.07×10^{-1}	4.41×10^{-1}	8.03×10^{-2}
14.0	0.659	-9.12×10^{-2}	9.66×10^{-1}	-4.31×10^{-1}	1.18×10^{-2}	3.41×10^{-2}	3.15×10^{-1}	-2.94×10^{-1}	1.52×10^{-2}	-2.63×10^{-1}	1.28×10^{-1}	5.78×10^{-2}
16.0	0.665	-8.07×10^{-2}	9.75×10^{-1}	-3.74×10^{-1}	1.12×10^{-2}	2.59×10^{-2}	3.24×10^{-1}	-3.42×10^{-1}	1.83×10^{-2}	-3.03×10^{-1}	-4.54×10^{-2}	3.84×10^{-2}
18.0	0.670	-7.22×10^{-2}	9.81×10^{-1}	-3.31×10^{-1}	9.92×10^{-3}	2.02×10^{-2}	2.83×10^{-1}	-3.78×10^{-1}	2.07×10^{-2}	-3.32×10^{-1}	-1.33×10^{-1}	2.54×10^{-2}
2.0×10^{1}	0.673	-6.53×10^{-2}	9.85×10^{-1}	-2.97×10^{-1}	8.47×10^{-3}	1.62×10^{-2}	2.65×10^{-1}	-4.05×10^{-1}	2.25×10^{-2}	-3.54×10^{-1}	-1.72×10^{-1}	1.70×10^{-2}
2.0×10^{2}	0.686	-6.67×10^{-3}	1.00	-2.92×10^{-2}	-3.16×10^{-3}	5.73×10^{-4}	3.13×10^{-2}	-5.37×10^{-1}	3.11×10^{-2}	-4.56×10^{-1}	9.38×10^{-3}	1.82×10^{-5}
2.0×10^{3}	0.686	-6.67×10^{-4}	1.00	-2.92×10^{-3}	-3.33×10^{-3}	5.61×10^{-5}	3.14×10^{-3}	-5.38×10^{-1}	3.12×10^{-2}	-4.57×10^{-1}	1.50×10^{-2}	1.62×10^{-6}
2.0×10^{4}	0.686	-6.67×10^{-5}	1.00	-2.92×10^{-4}	-3.33×10^{-3}	5.61×10^{-6}	3.14×10^{-4}	-5.38×10^{-1}	3.12×10^{-2}	-4.57×10^{-1}	1.51×10^{-2}	1.63×10^{-7}
2.0×10^{5}	0.686	-6.67×10^{-6}	1.00	-2.92×10^{-5}	-3.33×10^{-3}	5.61×10^{-7}	3.14×10^{-5}	-5.38×10^{-1}	3.12×10^{-2}	-4.57×10^{-1}	1.51×10^{-2}	1.66×10^{-8}
2.0×10^{6}	0.686	-6.67×10^{-7}	1.00	-2.92×10^{-6}	-3.33×10^{-3}	5.61×10^{-8}	3.14×10^{-6}	-5.38×10^{-1}	3.12×10^{-2}	-4.57×10^{-1}	1.51×10^{-2}	1.66×10^{-9}
∞	0.686	0.0	1.00	0.0	-3.33×10^{-3}	0.0	0.0	-5.38×10^{-1}	3.12×10^{-2}	-4.57×10^{-1}	1.51×10^{-2}	0.0

TABLE 1 (*a*). For caption see next page.

(b)

G_1	c_{0R}	c_{0I}	S_R	S_I	C_2	C_{2R}	C_3	C_{3R}	C_4	C_5	C_7	C_8
2.0×10^{-3}	0.458	-5.24×10^{-5}	-1.00	-9.16×10^{-4}	-5.74×10^{-2}	4.80×10^{-5}	-6.40×10^{-5}	-1.42×10^{-1}	-3.80×10^{-3}	2.30×10^{-1}	-6.27×10^{-3}	3.98×10^{-5}
2.0×10^{-2}	0.458	-5.24×10^{-4}	-1.00	-9.16×10^{-3}	-5.74×10^{-2}	4.80×10^{-4}	-6.40×10^{-4}	-1.42×10^{-1}	-3.80×10^{-3}	2.30×10^{-1}	-6.24×10^{-3}	4.02×10^{-4}
2.0×10^{-1}	0.458	-5.24×10^{-3}	-9.97×10^{-1}	-9.15×10^{-2}	-5.69×10^{-2}	4.74×10^{-3}	-6.28×10^{-3}	-1.41×10^{-1}	-3.77×10^{-3}	2.27×10^{-1}	-3.97×10^{-3}	3.90×10^{-3}
2.0	0.465	-5.30×10^{-2}	-7.02×10^{-1}	-8.35×10^{-1}	-3.47×10^{-2}	2.18×10^{-2}	-1.05×10^{-2}	-9.05×10^{-2}	-1.95×10^{-3}	1.10×10^{-1}	5.92×10^{-3}	-2.55×10^{-3}
4.0	0.490	-1.08×10^{-1}	4.11×10^{-3}	-1.24	-2.51×10^{-2}	1.94×10^{-2}	4.00×10^{-2}	-4.80×10^{-2}	-2.32×10^{-3}	6.55×10^{-2}	8.12×10^{-3}	-1.43×10^{-3}
6.0	0.548	-1.46×10^{-1}	6.29×10^{-1}	-1.09	-2.10×10^{-2}	2.24×10^{-2}	1.31×10^{-1}	-1.73×10^{-2}	-3.72×10^{-3}	4.70×10^{-2}	1.56×10^{-1}	-1.48×10^{-2}
7.0	0.555	-1.47×10^{-1}	6.66×10^{-1}	-1.06	-1.69×10^{-2}	2.39×10^{-2}	1.93×10^{-1}	-2.83×10^{-2}	-2.77×10^{-3}	1.29×10^{-2}	2.00×10^{-1}	-8.86×10^{-3}
7.2	0.561	-1.48×10^{-1}	6.99×10^{-1}	-1.03	-1.58×10^{-2}	2.40×10^{-2}	2.05×10^{-1}	-3.34×10^{-2}	-2.40×10^{-3}	4.03×10^{-3}	2.04×10^{-1}	-7.57×10^{-3}
7.4	0.567	-1.48×10^{-1}	7.28×10^{-1}	-9.94×10^{-1}	-1.48×10^{-2}	2.40×10^{-2}	2.16×10^{-1}	-3.93×10^{-2}	-1.97×10^{-3}	-5.27×10^{-3}	2.08×10^{-1}	-6.32×10^{-3}
7.6	0.573	-1.47×10^{-1}	7.54×10^{-1}	-9.63×10^{-1}	-1.39×10^{-2}	2.39×10^{-2}	2.27×10^{-1}	-4.59×10^{-2}	-1.49×10^{-3}	-1.49×10^{-3}	2.09×10^{-1}	-5.15×10^{-3}
7.8	0.579	-1.47×10^{-1}	7.76×10^{-1}	-9.33×10^{-1}	-1.30×10^{-2}	2.38×10^{-2}	2.37×10^{-1}	-5.31×10^{-2}	-9.82×10^{-4}	-2.48×10^{-2}	2.10×10^{-1}	-4.07×10^{-3}
8.0	0.584	-1.46×10^{-1}	7.96×10^{-1}	-9.04×10^{-1}	-1.21×10^{-2}	2.36×10^{-2}	2.46×10^{-1}	-6.08×10^{-2}	-4.40×10^{-4}	-3.48×10^{-2}	2.09×10^{-1}	-3.08×10^{-3}
8.2	0.590	-1.44×10^{-1}	8.13×10^{-1}	-8.77×10^{-1}	-1.13×10^{-2}	2.34×10^{-2}	2.55×10^{-1}	-6.90×10^{-2}	1.28×10^{-4}	-4.50×10^{-2}	2.07×10^{-1}	-2.20×10^{-3}
8.4	0.595	-1.43×10^{-1}	8.28×10^{-1}	-8.50×10^{-1}	-1.05×10^{-2}	2.31×10^{-2}	2.63×10^{-1}	-7.75×10^{-2}	7.16×10^{-4}	-5.51×10^{-2}	2.04×10^{-1}	-1.41×10^{-3}
8.6	0.599	-1.41×10^{-1}	8.41×10^{-1}	-8.26×10^{-1}	-9.74×10^{-3}	2.27×10^{-2}	2.71×10^{-1}	-8.62×10^{-2}	1.32×10^{-3}	-6.53×10^{-2}	2.00×10^{-1}	-7.23×10^{-4}
9.0	0.603	-1.40×10^{-1}	8.53×10^{-1}	-8.02×10^{-1}	-8.39×10^{-3}	2.20×10^{-2}	2.84×10^{-1}	-1.04×10^{-1}	2.55×10^{-3}	-8.52×10^{-3}	1.90×10^{-1}	3.89×10^{-4}
10.0	0.633	-1.21×10^{-1}	9.22×10^{-1}	-6.22×10^{-1}	-5.76×10^{-3}	1.99×10^{-2}	3.06×10^{-1}	-1.50×10^{-1}	5.64×10^{-3}	-1.32×10^{-1}	1.58×10^{-1}	1.95×10^{-3}
12.0	0.650	-1.04×10^{-1}	9.51×10^{-1}	-5.08×10^{-1}	-2.88×10^{-3}	1.58×10^{-2}	3.21×10^{-1}	-2.31×10^{-1}	1.11×10^{-2}	-2.09×10^{-1}	9.75×10^{-2}	2.39×10^{-3}
14.0	0.660	-9.11×10^{-2}	9.66×10^{-1}	-4.30×10^{-1}	-1.76×10^{-3}	1.26×10^{-2}	3.15×10^{-1}	-2.95×10^{-1}	1.53×10^{-2}	-2.65×10^{-1}	5.63×10^{-2}	1.88×10^{-3}
16.0	0.666	-8.06×10^{-2}	9.75×10^{-1}	-3.74×10^{-1}	-1.40×10^{-3}	1.02×10^{-2}	3.00×10^{-1}	-3.43×10^{-1}	1.85×10^{-2}	-3.05×10^{-1}	3.20×10^{-2}	1.36×10^{-3}
18.0	0.671	-7.21×10^{-2}	9.81×10^{-1}	-3.30×10^{-1}	-1.37×10^{-3}	8.50×10^{-3}	2.83×10^{-1}	-3.79×10^{-1}	2.09×10^{-2}	-3.34×10^{-1}	1.83×10^{-2}	9.17×10^{-4}
2.0×10^{1}	0.674	-6.53×10^{-2}	9.85×10^{-1}	-2.97×10^{-1}	-1.47×10^{-3}	7.22×10^{-3}	2.65×10^{-1}	-4.06×10^{-1}	2.27×10^{-2}	-3.56×10^{-1}	1.08×10^{-2}	7.18×10^{-4}
2.0×10^{2}	0.687	-6.66×10^{-3}	1.00	-2.91×10^{-2}	-3.21×10^{-3}	4.92×10^{-4}	3.13×10^{-2}	-5.38×10^{-1}	3.13×10^{-2}	-4.58×10^{-1}	1.45×10^{-2}	1.60×10^{-5}
2.0×10^{3}	0.687	-6.66×10^{-4}	1.00	-2.91×10^{-3}	-3.24×10^{-3}	4.89×10^{-5}	3.13×10^{-3}	-5.39×10^{-1}	3.13×10^{-2}	-4.59×10^{-1}	1.50×10^{-2}	1.58×10^{-6}
2.0×10^{4}	0.687	-6.66×10^{-5}	1.00	-2.91×10^{-4}	-3.24×10^{-3}	4.89×10^{-6}	3.13×10^{-4}	-5.39×10^{-1}	3.14×10^{-2}	-4.59×10^{-1}	1.50×10^{-2}	1.58×10^{-7}
2.0×10^{5}	0.687	-6.66×10^{-6}	1.00	-2.91×10^{-5}	-3.24×10^{-3}	4.89×10^{-7}	3.13×10^{-5}	-5.39×10^{-1}	3.14×10^{-2}	-4.59×10^{-1}	1.50×10^{-2}	1.58×10^{-8}
2.0×10^{6}	0.687	-6.66×10^{-7}	1.00	-2.91×10^{-6}	-3.24×10^{-3}	4.89×10^{-8}	3.13×10^{-6}	-5.39×10^{-1}	3.14×10^{-2}	-4.59×10^{-1}	1.50×10^{-2}	1.58×10^{-9}
∞	0.686	0.0	1.00	0.0	-3.33×10^{-3}	0.0	0.0	-5.38×10^{-1}	3.12×10^{-2}	-4.57×10^{-1}	1.51×10^{-2}	0.0

TABLE 1. (*a*) Table of coefficients for the phase-speed expression (6.61) and for the growth-rate expression (6.62). The slip coefficient κ is 10^{-3}. The label ∞ in the G_1 column corresponds to the coefficients obtained through an asymptotic analysis for $G_1 = \infty$. Here $D = 1.0$. (*b*) Same as (*a*) except that κ is 10^{-3}.

require the slip coefficient κ to be so small that the phase speed is only slightly affected. This is reasonable since we want the effects of slip to be local to the contact lines. Therefore, we restrict κ to be less than 0.01 so that $c_{0\mathrm{R}}$ varies less than 3% as κ varies from zero to 0.01. Greenspan (1978) also chooses the value 0.01 as an upper bound for his slip coefficient. Table 1 (*a*) gives results for $\kappa = 0.001$. In comparison with table 1 (*a*), where $\kappa = 10^{-8}$, we see that $c_{0\mathrm{R}}$, and $c_{0\mathrm{I}}$, vary negligibly as shown in figures 2 and 3.

Now after one integration of (6.50) and the applying of the boundedness condition we have the following differential equation to solve for h_1:

$$h_{1ZZZ} = -72SDZ - \frac{\mathrm{i}B_L}{D}\left[\frac{(1-c_0)Z - (\frac{1}{5}+(9S/35))Z^3 + \frac{1}{7}SZ^5}{\frac{1}{3}(1-Z^2)^2+\kappa}\right], \tag{6.53}$$

subject to conditions (6.15) and (6.38). At this point, though, c_1 in (6.38) is unknown. However, we can in principle integrate (6.53) three times and apply the boundary conditions (6.15) and (6.38) to determine h_1 in terms of c_1.

Upon completing this integration we find that restrictions must be placed upon the slip coefficient κ in order that our asymptotic expansions be uniformly valid. In particular we need that

$$\max(\mathrm{e}^{-\gamma}, \Phi) \ll \kappa < 0.01, \tag{6.54}$$

where

$$\gamma = \frac{DS}{B_d}, \tag{6.55}$$

$$\Phi = \left(\frac{B_d\beta}{DS}\right)^2. \tag{6.56}$$

Here β is a coefficient depending upon G_1 such that β decreases monotonically from a value of $\frac{16}{35}$ at $G_1 = 0$ to $\frac{1}{7}(3\kappa)^{\frac{1}{2}}$ at $G_1 = \infty$. See Appendix A for details. For values of B_d near 0.05 we find that restriction (6.54) is satisfied for

$$10^{-8} < \kappa < 10^{-3}. \tag{6.57}$$

Thus we place the lower bound restriction on the slip coefficient κ in order that our expressions for pressure, curvature, contact angle, and interface shape are mathematically well-defined quantities, and we place the upper bound restriction in order that slip effects be confined to the contact-line region.

Now, as before, solving (6.12*a*) subject to condition (6.12*c*) allows us to determine p_4 in terms of the unknown h_2. We then solve for the velocity components u_1, v_1, and w_1, and substitute them into the kinematic condition (6.5*e*). This results in a fourth-order differential equation in the transverse variable Z for h_2. The boundary conditions are (6.15), (6.39) and the bounded-velocity condition. This equation is solved numerically using the computer package SUPORT; see Scott & Watts (1977). We thus determine the eigenvalue correction

$$c_1 = [C_{2\mathrm{R}}B_L + C_{3\mathrm{R}}] + \mathrm{i}[C_2 B_L + C_3], \tag{6.58}$$

where the C_i and $C_{i\mathrm{R}}$ are numerical coefficients. Table 1 gives values for these as G_1 varies from the fixed-contact-angle to the fixed-contact-line regime.

The stability criterion at this stage is

$$c_{\mathrm{I}} = c_{0\mathrm{I}} + k^{\frac{1}{2}}[C_2 B_L + C_3] + O(k), \tag{6.59}$$

and so as before we need to go to higher order to obtain kinematic terms. Thus we shall use the short cut described in obtaining (6.28) in order to determine c_2. First

we solve for u_2 and h_2. From (6.39) we notice that h_2 depends on c_2 just as h_1 depended on c_1. The analysis for separating this dependence follows the same as that for h_1.

As before we set (6.28) equal to zero. The integrations in (6.28) are done numerically using Simpson's rule. Satisfying the two conditions stated in (6.28), we obtain the eigenvalue correction c_{2I}. We find that

$$c_{2I} = C_4 R + C_5 B_L^{-1} + C_7 B_L + C_8 B_L^2 + C_9, \tag{6.60}$$

where the C_i are numerical coefficients depending on G_1. In table 1 numerical values are given for these coefficients. The contribution from C_9 is negligible compared to those of c_{0I} and $k^{\frac{1}{2}} C_3$ for small k and thus is not listed.

In summary for the case of rivulets with moving contact lines and widths related to wavenumber as in relation (6.31) we have the disturbance phase speed

$$c_R = c_{0R} + k^{\frac{1}{2}}[C_{2R} B_L + C_{3R}] + O(k), \tag{6.61}$$

and flat rivulets on vertical walls being stable to small long-wave disturbances as long as $c_I < 0$, where

$$c_I = c_{0I} + k^{\frac{1}{2}}[C_2 B_L + C_3] + k[C_4 R + C_5 B_L^{-1} + C_7 B_L + C_8 B_L^2] + O(k^{\frac{3}{2}}), \tag{6.62}$$

with all coefficients listed in table 1.

We note that $B_d = B_L D k^{\frac{1}{2}}$ is chosen small enough in (6.62) so that restriction (6.54) is satisfied for $\kappa = 10^{-3}$ and $\kappa = 10^{-8}$. We could allow larger values for B_d when $\kappa = 10^{-3}$ but choose not to for comparison purposes. Table 1 shows that the neutral curves are nearly indistinguishable for G_1 greater than 8.2. We note here that if we were to continue the analysis to obtain corrections to relation (6.62) at order $k^{\frac{3}{2}}$, an examination of (5.4f) reveals that streamwise curvature effects proportional to $C_6 k^{\frac{1}{2}} B_d^{-1} = C_6 \bar{B}_d^{-1}$ would appear.

7. Results

We now consider the expression (6.62) for the growth rate c_I. The signs of the coefficients C_i and c_{0I} determine whether the terms are stabilizing (−) or destabilizing (+) to the system. We note that $c_{0I} + k^{\frac{1}{2}} C_3$ and $(k^{\frac{1}{2}} C_2 + k C_7) B_L$ are always negative so that the main prediction is that of stability. However, C_4 and C_5 change sign and, consistent with the perturbation nature of result (6.62), the system can be made less stable. However, if we were to push (6.62) beyond its expected range of validity by considering larger values of k, then c_I may become positive, implying instability. Such information can be *suggestive* in understanding the physical mechanisms present in the system.

For the latter reason we consider the following three rivulet flow regimes: $0 \leqslant G_1 < 7.4$, $7.4 \leqslant G_1 < 8.4$, and $8.4 \leqslant G_1 < \infty$. In the first region, $0 \leqslant G_1 < 7.4$, G_1 is small enough that we are describing 'narrow' rivulets with fixed contact angle and very mobile contact lines. Here $C_4 < 0$ and $C_5 > 0$ so that surface-tension effects are destabilizing to the system whereas flow effects are stabilizing. Such a situation may lead to a capillary instability in the rivulet, resulting in the rivulet breaking up into drops in much the same way as a capillary jet. This behaviour was seen by Culkin (1981) in his rivulet experiments. In figure 4 we plot the expression (6.62) for c_I versus the wavenumber k. The dashed portions of the curve denote the regions where the asymptotic expansion (6.62) may be breaking down since the $O(k)$ terms are becoming comparable to those of $O(k^{\frac{1}{2}})$. Figure 4 shows that as the mobility of the contact lines decreases or as the rivulet becomes wider (both cases corresponding to larger G_1) the

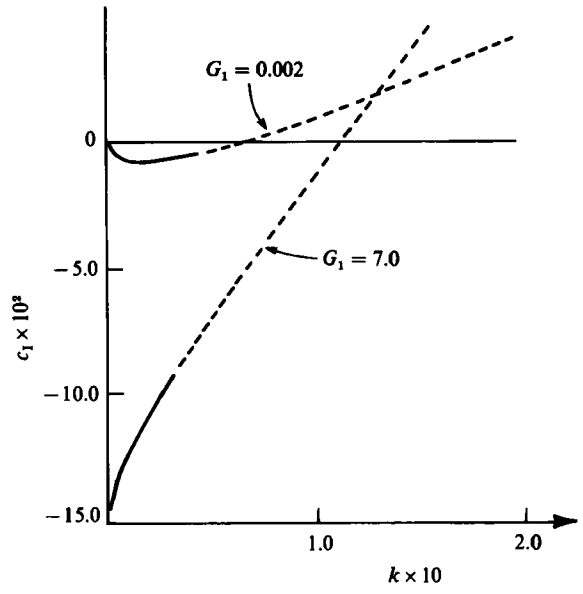

FIGURE 4. Plot of the growth rate expression (6.62) using values from table 1 describing a 'narrow' rivulet with very mobile contact lines ($G_1 = 0.002$) and a wider rivulet with less mobile contact lines ($G_1 = 7.0$). Here $R = 15.0$ and $B_L^* = 0.75$. The dashed portions denote where the asymptotic expansion (6.62) may no longer be valid.

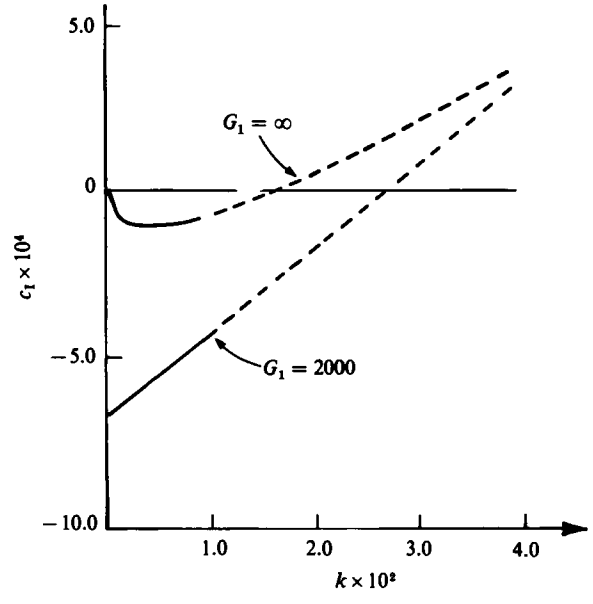

FIGURE 5. Plot of the growth rate expression (6.62) using values from table 1 describing a fixed contact line rivulet ($G_1 = \infty$) and a narrower rivulet with more mobile contact lines ($G_1 = 2000$). Here $R = 15.0$ and $B_L = 1.0$. The dashed portions denote where the asymptotic expansion (6.62) may no longer be valid.

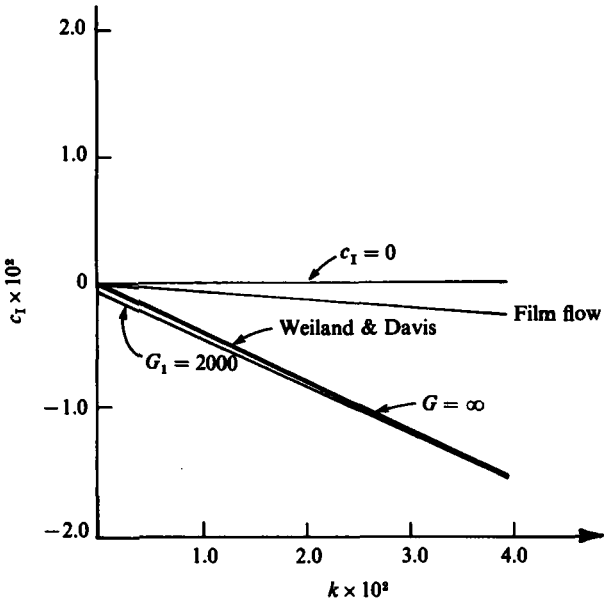

FIGURE 6. A comparison of the growth rate expressions for a film flow with a rivulet flow. The results found by Weiland & Davis (1981) are nearly indistinguishable from our fixed contact line result. Here $R = 2.0$ and $B_L = 1.0$.

region of stability increases; it is more difficult for the contact lines to approach each other and pinch the rivulet.

In the second region, $7.4 \leqslant G_1 < 8.4$, both C_4 and C_5 are negative. Thus flow effects and capillary effects are both stabilizing to the system. Here $c_I < 0$ and it appears for rivulets of width and contact-line mobility characterized by G_1 in the above region, that the basic-state straight rivulet is stable to small amplitude disturbances. J. Kern (1975 unpublished) and Culkin (1981) also find experimentally a region of flow rates within which the straight rivulet is stable to even large amplitude disturbances.

Finally, in the third region, $8.4 \leqslant G_1 < \infty$, $C_4 > 0$ and $C_5 < 0$ so that flow effects are destabilizing whereas capillary effects are stabilizing. This behaviour more closely resembles that of a film flow. Since G_1 is large in the above region, then we are describing very wide rivulets with rather immobile or even fixed contact lines. In figure 5 we plot the expression (6.62) for a fixed contact-line rivulet and for a less-wide rivulet with rather immobile contact lines ($G_1 = 2000$). It is seen that the narrower rivulet with mobile contact lines is more stable, implying that mobility may have a stabilizing effect on film flow instability.

In figures 6 to 8 we compare the growth rate expressions c_I for small amplitude, two-dimensional, long-wave disturbances in film flow, given by Yih (1963), and the expression found by Weiland & Davis (1981) for fixed contact-line rivulet instabilities with the results we show in figure 5. Yih (1963) gives (in our notation)

$$c_I = \tfrac{2}{15}k(R - \tfrac{5}{2}B_L^{-1}), \tag{7.1}$$

while Weiland & Davis (1981) find that

$$c_I = 0.031(R - 14.8B_L^{-1}). \tag{7.2}$$

In figure 6 for $R = 2.0$ and $B_L = 1.0$, all four expressions predict stability. In figure 7 for $R = 5.0$ and $B_L = 1.0$, only the film flow is predicted to be unstable. This is

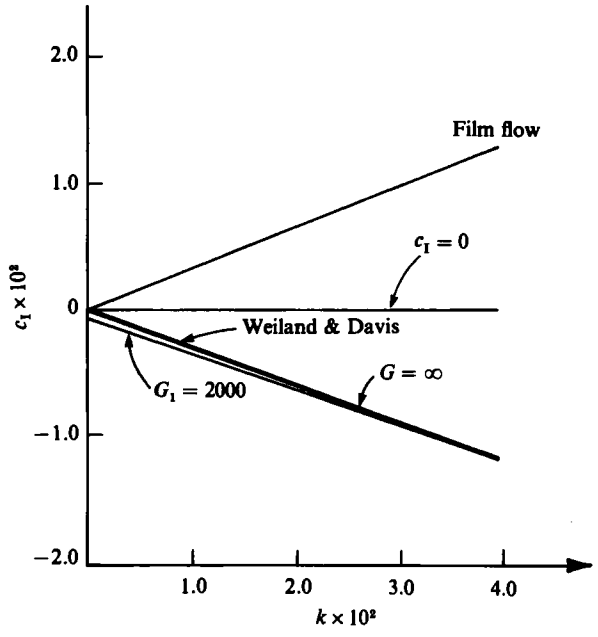

FIGURE 7. A comparison of the growth rate expressions for a film flow with a rivulet flow. The results found by Weiland & Davis (1981) are nearly indistinguishable from our fixed contact line result. Here $R = 5.0$ and $B_L = 1.0$.

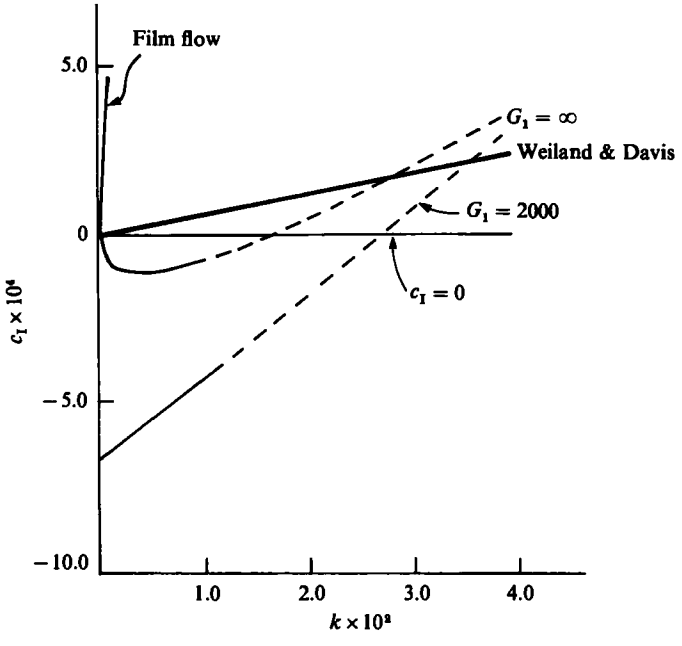

FIGURE 8. A comparison of the growth rate expressions for a film flow with a rivulet flow. Here $R = 15.0$ and $B_L = 1.0$. The dashed portions denote where the asymptotic expansion (6.62) may no longer be valid.

because the stabilizing capillary effects are stronger in rivulets due to the presence of the curved meniscus. In figure 8 for $R = 15.0$ and $B_L = 1.0$ all four expressions predict instability though the k is large enough that our asymptotics may no longer be valid. We see that the presence of the contact lines makes the rivulet stable to small amplitude disturbances at very small wavenumber. In this region film flow is unstable and Weiland & Davis (1981) predict rivulet instability with $k = 0$ being a neutrally stable state.

8. Discussion and summary

We consider the flow of a rivulet down a vertical wall. The ratio δ of the maximum rivulet height to the maximum half width of the rivulet is assumed to be small. We allow slip between the liquid and the solid surface at the contact line using a Navier slip model with a slip coefficient inversely proportional to the height of the interface. We consider long-wave disturbances having wavenumber k. When $\delta \ll 1$ and $k \ll 1$, we examine a linear stability analysis of the basic straight rivulet by assuming $\delta^2 = O(k^s)$. This family of problems divides into three categories:

(i) $\delta \gg k$; $s < 2$ $\rightarrow \dfrac{\delta^2}{B_d} = \dfrac{1}{B_L} = O(1)$ 'narrow',

(ii) $\delta = k$; $s = 2$ $\rightarrow \dfrac{k^2}{B_d} = \dfrac{\delta^2}{B_d} = O(1)$,

(iii) $\delta \ll k$; $s > 2$ $\rightarrow \dfrac{k^2}{B_d} = O(1)$ wide.

Here the parameter s measures the relative degree of the width of the flat, wide rivulet. In case (i) the rivulet is narrow enough that cross-stream curvature effects dominate streamwise curvature effects. In case (ii) the two effects are comparable, while in case (iii) streamwise curvature effects are the more important. For the limiting case, $s \rightarrow \infty$, we obtain results for an infinitely wide rivulet, which is equivalent to a two-dimensional film flow. In fact for $s > 2$, the film-flow approximation is valid (Young 1985). Long-wave disturbances are realized through the usual normal-mode assumption. Hysteresis is not included in the analysis since it cannot be retained upon linearization (Davis 1980). Therefore we allow the contact angle θ to be a linear function of the contact-line speed U_{CL}, namely $\theta = \phi + G'(0)\, U_{\mathrm{CL}}$. The static angle ϕ measures the *wettability* of the solid and the slope $G'(0)$ measures the *mobility* of the contact lines. When $G'(0)$ is small, the contact lines are very mobile and $G'(0) \rightarrow 0$ gives the fixed-contact-angle case. When $G'(0)$ is large, the contact lines are very immobile and $G'(0) \rightarrow \infty$ gives the fixed-contact-line case. In our formulation we introduce the parameter G_1 in (6.35), proportional to $G'(0)$, to measure the importance of the rivulet width and the mobility of the contact lines. We see that large G_1 can describe either a very wide rivulet or a rivulet with almost fixed contact lines. Likewise, small G_1 corresponds to a narrower rivulet or one with very mobile contact lines.

We perform an asymptotic analysis of the linearized disturbance equations. For the case of fixed contact lines, all results can be obtained analytically. For the case of mobile contact lines we need to integrate some quantities numerically. We use the asymptotic results as a check on the numerical results.

Our results can best be summarized through the expression (6.62) for the growth rate c_{I}. This expression for the case $s = \frac{1}{2}$ can be simplified by neglecting the terms of orders $k B_L$ and $k B_L^2$. The result is as follows:

$$c_{\mathrm{I}} = C_1 + k^{\frac{1}{2}}[C_2 B_L + C_3] + k[C_4 R + C_5 B_L^{-1}] + k^{\frac{3}{2}} C_6 \tilde{B}_d^{-1}, \tag{8.1}$$

or equivalently

$$c_{\mathrm{I}} = C_1 + C_2 B_d + k^{\frac{1}{2}} C_3 + k[C_4 R + C_5 B_L^{-1}] + k^{\frac{3}{2}} C_6 \tilde{B}_d^{-1}, \tag{8.2}$$

where $C_1 = c_{0\mathrm{I}}$. Here C_1 to C_6 are functions depending strongly upon G_1 and weakly upon the slip coefficient κ. B_d is a Bond number based upon the maximum height of the rivulet. B_L is a Bond number based upon the maximum half-width of the rivulet, and R is the Reynolds number. Stability is obtained when $c_{\mathrm{I}} < 0$. We have shown that c_{I} is composed of four contributions:

1. $C_1 + k^{\frac{1}{2}} C_3$ → contact-angle effects;
2. $C_5 B_L^{-1}$, $C_6 \tilde{B}_d^{-1}$ → capillary effects;
3. $C_2 B_L$ → contact-line effects;
4. $C_4 R$ → flow effects.

C_1 to C_6 depend weakly upon the amount of slip between the liquid and the solid at the contact line. On one hand, κ should be small enough that the bulk flow is unaffected by the presence of slip near the contact lines. On the other hand, κ should be large enough that the force singularity is appropriately removed. Our results show that it is the value of $\log \kappa$ which emerges, as expected from the results by Hocking (1977, 1983), and Greenspan (1978) for other problems. Within the range of κ 10^{-8} to 10^{-3}, we find that C_1 to C_5 are nearly independent of slip; presumably the same holds for C_6.

For the case $s = \frac{1}{2}$, C_1 to C_6 are strongly dependent on the width of the rivulet and the mobility of the contact lines, both of which are characterized by G_1. Equations (8.1) and (8.2) apply with the coefficients listed in table 1. If one wishes to examine rivulets that are much wider than the class considered, one must allow larger values of s. For $1 < s < 2$ Young (1985) develops nonlinear evolution equations for $h(x, z, t)$ and from these finds the equivalents of C_1 to C_6, as discussed below. Young (1985) also considers $s \geqslant 2$ and finds that $s = 2$ is the asymptotic equivalent of the 'widest' rivulet-film flow. We now discuss the full range of G_1 and s, using in part results obtained by Young (1985).

C_1 to C_6 are strongly dependent on s and G_1, and thus are strongly dependent on the width of the rivulet and the mobility of the contact lines. We find the following behaviour for each:

$C_1 + k^{\frac{1}{2}} C_3$ negative for all G_1; proportional to G_1, for small G_1 and proportional to G_1^{-1} for large G_1; $C_1 + k^{\frac{1}{2}} C_3 \to 0$ as $s \to \infty$.

C_2 negative for all G_1 and such that $|C_2|$ decreases monotonically as $G_1 \to \infty$; $C_2 \to 0$ as $s \to \infty$.

C_4 negative for small G_1 and positive for large G_1; C_4 approaches the film-flow value as $s \to \infty$.

C_5 positive for small G_1 and negative for large G_1; C_5 approaches zero as $s \to \infty$.

C_6 approaches the film-flow value as $s \to \infty$. (All results for C_6 are obtained through a consideration of a nonlinear evolution equation developed for wider rivulets, Young 1985.)

One must be cautious in taking the limit $s \to \infty$ to get film flow since the presence of the contact lines and the contact-line boundary conditions make this a singular limit.

We interpret the above results as follows for each of the effects (1)–(4).

1. *Contact-angle effects.* The contact angle increases with advancing contact-line speed or decreases with receding contact-line speed. This effect together with the contact-line effects is always stabilizing to the system. This effect weakens when the contact angle is nearly fixed and when the contact line is nearly fixed, since for both these cases the contact angle is nearly independent of the contact-line speed. This effect is also negligible for wide enough rivulets.

2. *Capillary effects.* Corrugations of the interface produce pressure gradients driven by surface tension. These gradients are destabilizing, similar to those of the capillary instability of a jet, when the contact lines are very mobile, yet are stabilizing, similar to those of film flow, when the contact lines are fairly immobile. Likewise, as the rivulet widens, these effects become more like those in a film. Obviously, the presence of the solid surface distinguishes the film behaviour from the jet behaviour. Our results indicate that this difference can be overcome by increasing the mobility of the contact lines.

3. *Contact-line effects.* Regardless of the mobility $G'(0)$ of the contact lines, the *presence* of a contact line is always stabilizing. Wide rivulets are affected less by the presence of contact lines than the narrow ones.

In essence the capillary-effect (B_L^{-1} and B_d^{-1}) terms describe the surface-tension effects away from the contact lines and the contact-line effect (B_L) terms describe these effects near them. Rosenblat & Davis (1984) call the effects 'capillary push' and 'contact-line pull', respectively. For the case of fixed contact angle the two effects oppose one another in that the contact lines move to squeeze fluid into thinner regions whereas capillary pressures pump it out of these regions. If capillary pressures win, then thick portions of the rivulet tend to swell. The contact angle in these portions becomes larger than the static angle and so the contact lines advance as shown in figure 9. The opposite occurs in the thinner portions; these sections shrink, the contact angle is smaller than the static angle, and so the contact lines recede. The result is that drops are pinched from the rivulet. On the other hand, for very immobile contact lines (large G_1) both the 'capillary push' and 'contact-line' pull effects work to pump fluid into thinner regions. As shown in figure 9, thick portions shrink (thin portions swell) thus causing the contact angles to be less than (greater than) the static contact angle. Thus, the contact lines of the thicker portion recede and those of the thin, advance. The result is a stabilization of the rivulet to long-wave disturbances.

4. *Flow effects.* Increasing the flow rate tends to stabilize the capillary instabilities for small G_1 and enhance the kinematic-wave instabilities for large G_1.

We *conjecture* that these effects combine to give the following rivulet flow regimes. When the rivulet is 'narrow' and the contact lines are mobile, so that G_1 is small, the capillary effects can lead to a break-up instability. This instability can be overcome if the Reynolds number R is large enough. On the other hand when the contact lines are less mobile, so that G_1 is large, the capillary instability is suppressed because the contact lines can no longer move together and pinch off drops. Now the rivulet is susceptible only to a kinematic-wave instability which occurs at high flow rates. Here capillary effects oppose the instability while flow effects enhance it.

When the rivulet is wide, independent of the mobility of the contact lines, it is susceptible only to a kinematic-wave instability. The rivulet resembles a film and the bulk flow does not feel the motion of the contact lines. However, the presence of the

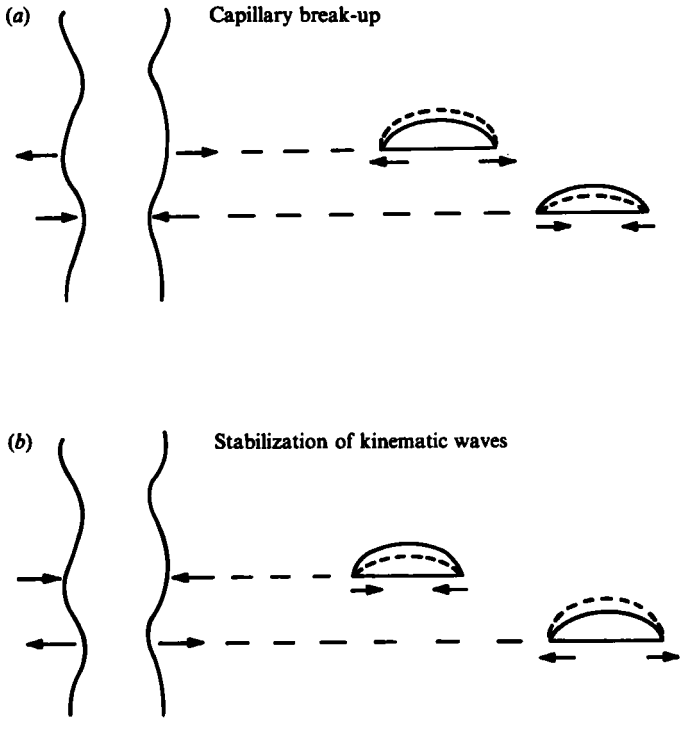

FIGURE 9. Contact line motion: (*a*) In the capillary break-up of a rivulet flow, fluid is pumped from thin regions into thick regions. The thick regions swell causing the contact lines to advance. The thin regions shrink causing the contact lines to recede; (*b*) When a rivulet is susceptible to a kinematic-wave instability, capillary pressures help to stabilize the rivulet by causing fluid to be pumped from thick regions into thin regions.

contact lines is felt so that the rivulet is more stable to long-wave disturbances than is film flow.

The effects of the contact lines are strongest as $k \to 0$. When G_1 is small, the capillary instabilities are weak for very long waves because the interface is nearly flat. Thus, unlike the jet, the rivulet flow is stable for very small wavenumbers. At the other extreme, for large G_1, the presence of the contact lines gives a region of unconditional stability for a rivulet, in contrast to that of a film flow.

We note that our analysis always predicts varicose instabilities and thus there is no prediction of rivulet meandering, a sinuous instability. The meandering rivulets observed by Culkin (1981) are rather narrow, $\delta \approx 0.9$. The resulting higher cross-stream curvature in his rivulets may lead to the side-to-side shimmering of the rivulet which he observes just before meandering takes place. This suggests the development of transverse waves across the rivulet width. We have not included hysteresis in our analysis. Since Culkin does not test any low hysteresis systems (because none were available), it has not been concluded that such rivulets can meander. If it were true that meandering depends upon the presence of hysteresis, then our obtaining only varicose instabilities rather than sinuous instabilities would be consistent with the no-hysteresis assumption. It may also be true that meandering is an instability from a disturbed state different from the straight rivulet and it represents a secondary instability.

This work was supported by a grant from the National Science Foundation, Fluid Mechanics Program.

Appendix A

In order that our asymptotic expansions for pressure, curvature, contact angle, and interfacial shape are mathematically well defined, we require that restrictions be placed upon the slip coefficient κ. Upon integrating (6.53) once we find that

$$h_{1ZZ} = -36SDZ^2 + \frac{3iB_L}{2D}\left\{\tfrac{1}{7}S(1-Z^2) + \tfrac{1}{2}(\tfrac{1}{5}-\tfrac{1}{35}S)\log[(1-Z^2)^2+3\kappa]\right.$$
$$\left. + [\tfrac{4}{5}-c_0-\tfrac{4}{35}S-\tfrac{1}{7}S(3\kappa)^{\frac{1}{2}}](3\kappa)^{-\frac{1}{2}}\tan^{-1}\left(\frac{1-Z^2}{(3\kappa)^{\frac{1}{2}}}\right)\right\} + \tau, \quad \text{(A 1)}$$

where τ is a constant of integration.

We now consider the pressure field

$$p = k\frac{2S}{B_L} + k^{\frac{3}{2}}\frac{3i}{2D}\left\{\tfrac{1}{2}(\tfrac{1}{5}-\tfrac{1}{35}S)\log[(1-Z^2)^2+3\kappa]\right.$$
$$\left. + [\tfrac{4}{5}-c_0-\tfrac{4}{35}S-\tfrac{1}{7}S(3\kappa)^{\frac{1}{2}}](3\kappa)^{-\frac{1}{2}}\tan^{-1}\left(\frac{1-Z^2}{(3\kappa)^{\frac{1}{2}}}\right)+\tau\right\}, \quad \text{(A 1}a\text{)}$$

obtained from (6.40), (6.43) and (A 1). We have neglected terms which are bounded at the contact lines at order $k^{\frac{3}{2}}$. The constant of integration τ is determined through the boundary conditions (6.15) and (6.39) in a later analysis and it is found that τ is proportional to

$$-[\tfrac{4}{5}-c_0-\tfrac{4}{35}S-\tfrac{1}{7}S(3\kappa)^{\frac{1}{2}}](3\kappa)^{-\frac{1}{2}}\tan^{-1}\left(\frac{1}{(3\kappa)^{\frac{1}{2}}}\right). \quad \text{(A 2)}$$

Now form (A 1a) will be uniformly valid as long as

$$k^{\frac{1}{2}}\log[(1-Z^2)^2+3\kappa] \ll \frac{S}{B_L}, \quad \text{(A 3)}$$

which restricts the size of the slip coefficient so that

$$\kappa \gg \exp[-\gamma], \quad \text{(A 4)}$$

where

$$\gamma = \frac{S}{k^{\frac{1}{2}}B_L} = \frac{DS}{B_d}, \quad \text{(A 5)}$$

where we have used relation (6.9). In addition, we must also have

$$k^{\frac{1}{2}}\beta(3\kappa)^{-\frac{1}{2}}\tan^{-1}\left(\frac{1}{(3\kappa)^{\frac{1}{2}}}\right) \ll \frac{S}{B_L}, \quad \text{(A 6)}$$

so that we need

$$\kappa \gg \frac{kB_L^2\beta^2}{S^2} = \frac{B_d^2\beta^2}{D^2S^2} \equiv \Phi. \quad \text{(A 7)}$$

In this expression β is given by

$$\beta = [\tfrac{4}{5}-c_0-\tfrac{4}{35}S-\tfrac{1}{7}S(3\kappa)^{\frac{1}{2}}], \quad \text{(A 8)}$$

and in arriving at this expression we have used the principal value for the $\tan^{-1}\psi$, $-\frac{1}{2}\pi < \tan^{-1}\psi < \frac{1}{2}\pi$.

We must satisfy conditions (A 4) and (A 7) simultaneously. From (A 5) we see that if the Bond number B_d is small then γ will be large so that $e^{-\gamma}$ is extremely small. Thus, we can pick B_d small enough so that

$$e^{-\gamma} \ll \Phi, \tag{A 9}$$

and therefore satisfying condition (A 7) automatically satisfies (A 4).

The relation (A 8) shows that β decreases monotonically from a value of $\frac{16}{35}$ at $G_1 = 0$, to $\frac{1}{7}(3\kappa)^{\frac{1}{2}}$ at $G_1 = \infty$. In fact for $G_1 > 14$, $\beta \approx \frac{1}{7}(3\kappa)^{\frac{1}{2}}$. If we substitute this value for β into relation (A 7), we obtain

$$\tfrac{49}{3} D^2 S^2 \gg B_d^2. \tag{A 10}$$

Since table 1 shows that S^2 is $O(1)$ and D is also by definition $O(1)$, then relation (A 10) is easily satisfied for B_d not too small. Thus, as long as $G_1 > 14$, then condition (A 7) is satisfied for extremely small values of κ and condition (A 4) is the only (rather weak) restriction on κ. For example if $B_d = 0.1$ and $DS = 1.7$, then $\kappa > 10^{-7}$. This agrees with our modelling assumptions about slip, since the larger G_1 is, the less mobile are the contact lines. Therefore, one would expect that less slip is required.

However, if $G_1 < 14$, then $\beta \approx \frac{16}{35}$ so condition (A 7) becomes

$$\kappa \gg \frac{0.2 B_d^2}{D^2 S^2}. \tag{A 11}$$

Now if $DS = 1.7$ and $B_d = 0.1$ as before, then we require that $\kappa \gg 10^{-4}$. Thus, we need larger slip near the contact lines. But in either case, whether G_1 is large or small, we can still satisfy

$$\max(e^{-\gamma}, \Phi) \ll \kappa < 0.01, \tag{A 12}$$

for a wide range of values of B_d and keep κ small enough that its effects are felt only near the contact lines.

In summary, we place the lower bound restriction (A 12) on the slip coefficient κ in order that our expressions for pressure, curvature, contact angle, and interfacial shape are mathematically well-defined quantities, and we place the upper bound restriction in order that slip effects be confined to the contact-line region. Greenspan (1978) also recognizes that such restrictions are necessary when considering the spreading of a drop on a horizontal solid. However, he poses only condition (A 4) as the lower bound since he expands only contact angle and interfacial shape. Yet if one differentiates the expression (A 3) of his Appendix, terms of the form

$$\frac{1}{\lambda} \tan^{-1}\left(\frac{1}{\lambda}\right) \tag{A 13}$$

appear where his λ is our $(3\kappa)^{\frac{1}{2}}$. Since his expression (A 3) is the derivative of the interfacial shape, then its derivative is the curvature. Thus, the restriction (A 7) must also be applied to his problem in order that interfacial curvature be well-defined mathematically. We note that if $\kappa \to 0$ in (6.53), then h_{1ZZ} will not only have logarithmic terms but also terms proportional to

$$\frac{1}{1-Z^2}. \tag{A 14}$$

These lead to non-uniform expansions when $1 \pm Z = O(k^{\frac{1}{2}})$. If (6.53) is rewritten as

$$[\tfrac{1}{3}(1-Z^2)^2 + \kappa)\, h_{1ZZZ} = h_{1\text{particular}}, \tag{A 15}$$

we see that $\kappa = 0$ means that (A 15) is a singular differential equation at the contact lines $Z = \pm 1$. Thus slip is needed to relieve the singularity shown in (A 14). Slip serves the dual role of relieving a multi-valued velocity field at the contact line, and allowing for a bounded pressure field there. The latter role appears to be peculiar to problems where the fluid thickness approaches zero, as at the contact lines in our model and in the Greenspan (1978) model. Similarly, Silliman & Scriven (1978) find in their finite element analysis of a die swell at a channel exit, that the pressure decreases near the contact-line region as the slip coefficient increases. Hocking (1977) also finds that the pressure drop required to cause the flow of two immiscible fluids through a capillary, decreases as the slip coefficient increases.

REFERENCES

Allen, R. F. & Biggin, C. M. 1974 *Phys. Fluids* **17**, 287.

Atherton, R. W. & Homsy, G. M. 1976 *Chem. Engng Commun.* **2**, 57.

Benjamin, T. B. 1957 *J. Fluid Mech.* **2**, 554.

Benney, D. J. 1966 *J. Maths & Phys.* **45**, 150.

Culkin, J. B. 1981 Rivulet meandering. Ph.D. thesis, Northwestern University, Evanston, Illinois.

Davis, S. H. 1980 *J. Fluid Mech.* **98**, 225.

Dussan V., E. B. 1976 *J. Fluid Mech.* **77**, 665.

Dussan V., E. B. 1979 *Ann. Rev. Fluid Mech.* **11**, 371.

Dussan V., E. B. & Chow, R. T.-P. 1983 *J. Fluid Mech.* **137**, 1.

Dussan V., E. B. & Davis, S. H. 1974 *J. Fluid Mech.* **65**, 71.

Greenspan, H. P. 1978 *J. Fluid Mech.* **84**, 125.

Hocking, L. M. 1977 *J. Fluid Mech.* **79**, 209.

Hocking, L. M. 1983 *Q. J. Mech. Appl. Maths.* **36**, 55.

Kern, J. 1969 *Verfahrenstechnik* **3**, 425.

Kern, J. 1971 *Verfahrenstechnik* **5**, 289.

Krantz, W. B. & Goren, S. L. 1970 *I and EC Fundamentals* **9**, 107.

Ngan, C. C. & Dussan V., E. B. 1982 *J. Fluid Mech.* **118**, 27.

Rayleigh, Lord 1879 *Proc. R. Soc. Lond.* A **10**, 4.

Rosenblat, S. & Davis, S. H. 1984 *Frontiers in Fluid Mechanics* (ed. S. H. Davis & J. L. Lumley), p. 171. Springer.

Scott, M. R. & Watts, H. A. 1977 *SIAM J. Num. Anal.* **14**, 40.

Silliman, W. J. & Scriven, L. E. 1978 *Phys. Fluids* **21**, 2115.

Towell, G. D. & Rothfeld, L. B. 1966 *AIChE J.* **12**, 972.

Weiland, R. H. & Davis, S. H. 1981 *J. Fluid Mech.* **107**, 261.

Yih, C.-S. 1963 *Phys. Fluids* **6**, 321.

Young, G. W. 1985 Dynamics and stability of flows with moving contact lines. Ph.D. thesis, Northwestern University, Evanston, Illinois.

Young, G. W. & Davis, S. H. 1985 *Q. Appl. Maths* **42**, 403.